Research Paper

PAIN®

Abnormal activity of corneal cold thermoreceptors underlies the unpleasant sensations in dry eye disease

Illés Kovács[a,b], Carolina Luna[a], Susana Quirce[a], Kamila Mizerska[a], Gerard Callejo[c,d], Ana Riestra[e], Laura Fernández-Sánchez[f], Victor M. Meseguer[a], Nicolás Cuenca[f], Jesús Merayo-Lloves[e], M. Carmen Acosta[a], Xavier Gasull[c,d], Carlos Belmonte[a,e], Juana Gallar[a,*]

Abstract

Dry eye disease (DED) affects >10% of the population worldwide, and it provokes an unpleasant sensation of ocular dryness, whose underlying neural mechanisms remain unknown. Removal of the main lachrymal gland in guinea pigs caused long-term reduction of basal tearing accompanied by changes in the architecture and density of subbasal corneal nerves and epithelial terminals. After 4 weeks, ongoing impulse activity and responses to cooling of corneal cold thermoreceptor endings were enhanced. Menthol (200 μM) first excited and then inactivated this augmented spontaneous and cold-evoked activity. Comparatively, corneal polymodal nociceptors of tear-deficient eyes remained silent and exhibited only a mild sensitization to acidic stimulation, whereas mechanonociceptors were not affected. Dryness-induced changes in peripheral cold thermoreceptor responsiveness developed in parallel with a progressive excitability enhancement of corneal cold trigeminal ganglion neurons, primarily due to an increase of sodium currents and a decrease of potassium currents. In corneal polymodal nociceptor neurons, sodium currents were enhanced whereas potassium currents remain unaltered. In healthy humans, exposure of the eye surface to menthol vapors or to cold air currents evoked unpleasant sensations accompanied by increased blinking frequency that we attributed to cold thermoreceptor stimulation. Notably, stimulation with menthol reduced the ongoing background discomfort of patients with DED, conceivably due to use-dependent inactivation of cold thermoreceptors. Together, these data indicate that cold thermoreceptors contribute importantly to the detection and signaling of ocular surface wetness, and develop under chronic eye dryness conditions an injury-evoked neuropathic firing that seems to underlie the unpleasant sensations experienced by patients with DED.

Keywords: Eye pain, Dry eye, Corneal nerve injury, Neuropathic pain, Eye inflammation, Cold thermoreceptors, Nociceptors

1. Introduction

The precorneal tear film that covers the exposed surface of the eye is continuously subjected to evaporation. Under normal circumstances, this fluid loss is replenished through the secretion of tears by the lachrymal glands, helping to moisten the nonkeratinized epithelium of the corneal surface.[17] Dry eye disease (DED) is a multifactorial ocular disease due in most cases to deficient tear production or excessive evaporation, resulting in discomfort, visual disturbance, and tear instability, with potential damage to the eye surface.[64] The peripheral neural mechanisms underlying the sensation of dryness elicited by abnormal ocular surface desiccation are poorly understood. During interblink periods, the temperature of the eye surface decreases rapidly because of tear evaporation.[68] Osmolality of the tear film also rises,[46] whereas thinning and eventual disruption of the precorneal tear film apply mechanical stress to the cells and nerve fibers of the superficial epithelial layers of the cornea,[27,56] eventually causing local release of inflammatory agents.[44] All these physical and chemical disturbances that accompany excessive evaporation represent potential stimuli for the distinct functional classes of trigeminal ganglion (TG) sensory neurons that innervate the ocular surface (mechanonociceptor, polymodal nociceptor, and cold thermoreceptor neurons),[10,24] each of which is a possible source of the discomfort evoked by eye surface dryness.[3,8,35,36,43] However, the relative contribution of these various neuron functional types to the final sensory input evoking unpleasant symptoms of dryness in healthy subjects and patients with DED are still largely ignored because the molecular mechanisms underlying the excitation of corneal peripheral endings during eye surface dryness in normal and pathological conditions are still unknown.

To address these questions, we experimentally reproduced in guinea pigs the reduced wetness of the ocular surface in DED through unilateral, surgical removal of the main lachrymal gland[42] and examined its effects on the morphology and impulse firing of

Sponsorships or competing interests that may be relevant to content are disclosed at the end of this article.

[a] *Instituto de Neurociencias, Universidad Miguel Hernández–CSIC, San Juan de Alicante, Spain,* [b] *Department of Ophthalmology, Semmelweis University, Budapest, Hungary,* [c] *Laboratory of Neurophysiology, Department of Biomedicine, School of Medicine, University of Barcelona, Barcelona, Spain,* [d] *Institut d'Investigacions Biomèdiques August Pi i Sunyer (IDIBAPS), Barcelona, Spain,* [e] *Instituto Universitario Fernández-Vega, Universidad de Oviedo and Fundación de Investigación Oftalmológica, Oviedo, Spain,* [f] *Departamento de Fisiología, Genética y Microbiología, Universidad de Alicante, San Vicente del Raspeig, Spain*

**Corresponding author. Address: Instituto de Neurociencias, Universidad Miguel Hernández-CSIC, Avenida Santiago Ramon y Cajal, s/n, 03550 San Juan de Alicante, Spain. Tel.: +34 965919532; fax: +34 965919549. E-mail address: juana.gallar@umh.es (J. Gallar).*

PAIN 157 (2016) 399–417

http://dx.doi.org/10.1097/j.pain.0000000000000455

corneal nerve fibers, as well as on the sodium and potassium membrane currents of the various functional classes of corneal sensory neurons. We also explored in humans the quality of the conscious sensations evoked by stimulation of cold sensory receptors of the ocular surface in healthy individuals and in patients with DED.

2. Methods

2.1. Animal experiments

Dunkin Hartley guinea pigs of both sexes weighing 200 to 300 g were used. Animals were kept in individual cages with free access to food and water and were maintained under controlled day–night cycles. The study was performed in accordance with the *NIH Guide for the Care and Use of Laboratory Animals*, the European Union Directive (2010/63/EU), and the Spanish regulations on the protection of animals used for research and followed a protocol approved and supervised by the Ethics Committees of the University Miguel Hernández and the University of Barcelona.

2.1.1. Surgical procedures

Animals were anaesthetized with ketamine (90 mg/kg i.p.) and xylazine (5 mg/kg i.p.) for unilateral removal of the main lachrymal gland. After performing an 8-mm skin incision on the temporal side, posterior to the lateral canthus, the fibrous capsule of the exorbital gland was exposed and dissected, and the lachrymal gland was carefully excised. Total removal was verified by inspecting the surgical area for any remaining glandular tissue. At the end of the operation, a drop of antibiotic (3 mg/mL tobramycin) was applied onto the surgical area. The skin incision was then sutured using 6.0 braided silk suture. Animals were housed individually, and conjunctival and corneal signs were checked regularly. Palpebral morphology and reflex blinking responses to corneal stimulation were tested postsurgically. Both appeared unaffected in all the operated animals. Diluted fluorescein dye (5 μL of 0.2% fluorescein; Alcon-Cusí, Barcelona, Spain) instilled in the eye was used to confirm the absence of corneal epithelial defects developed after lachrymal gland excision. In preliminary experiments, a group of guinea pigs were subjected to every step of the above-described procedure except the gland removal. No differences in tear secretion and corneal nerve activity were found between sham-operated and nonoperated animals. Thus, nonoperated guinea pigs of similar age and weight were used as the control group. Animals were randomly assigned to the experimental groups.

2.1.2. Tear secretion and blink rate measurement

Values of tear secretion and blink rate in the absence of intended stimulation (basal values) were determined before and at different times after surgery (1, 2, and 4 weeks) under stable environmental conditions (23°C temperature; 55% humidity). Blinks were independently counted during a 5-minute period, whereas the animal move freely in a 80 × 60 × 60 cm ceiling-less white cage by 2 different observers (one eye each observer) who knew the assignation of the animal to an experimental group. The number of scratching movements of the posterior legs directed to the either eye during this 5-minute period was also noted.[4]

Immediately after assessing the blink rate and eye-scratching movements, tear fluid secretion was measured in both eyes using commercial phenol red threads (Zone-Quick; Menicon, Tokyo, Japan) placed under the lower lid for 30 seconds without topical anesthesia.[4,72] The lower lid was pulled down slightly, the folded 2-mm end of the thread was gently placed onto the nasal palpebral conjunctiva, and the lower lid was released. After a 30-second period, the lower lid was again pulled down and the thread was gently removed. The length of the red thread reflects the measure of the tear volume in the conjunctival sac and tear secretion over the period of measurement. The tear rate was determined as the entire length of the red-stained portion of the thread in millimeters, measured with a ruler under a stereomicroscope with an accuracy of ±0.5 mm. The data obtained from control and operated animals at different time points after lachrymal gland removal were compared using the appropriate paired parametric or nonparametric statistical test, as indicated.

In a separate set of experiments, blink rate and scratching responses were measured during 5 minutes in control and 4-week tear-deficient guinea pigs, before and immediately after topical ocular application of 10 μL of cold saline (2°C), menthol (100-200 μM), and capsaicin (100 μM), and the tear rate was measured afterwards (ie, 5 minutes after topical treatment).[5] Ocular instillation of a 10 μL drop of warm saline (35°C) did not produce changes in the tear rate or blink frequency nor did it evoke eye-scratching response (data not shown). In this set of experiments, intervals of 40 to 90 minutes were allowed between applications of the different test solutions.

2.1.3. Immunohistochemistry of corneal nerves

The morphological changes of corneal nerves were analyzed 4 weeks after removal of the main lachrymal gland. Animals were killed with an overdose of anesthetic, and both eyes were excised. Eyeballs were fixed in 4% paraformaldehyde in 0.1 M phosphate buffer (PB), pH = 7.4, for 1 hour at room temperature. After washes in 0.1 M PB, eyes were cryoprotected in 10% sucrose for 1 hour and 20% sucrose for 1 hour, followed by immersion in 30% sucrose overnight. The next day, corneas were dissected from the eye cups and radial cuts were made to flatten them. Corneas were put through a freeze–thaw procedure by dipping them in liquid nitrogen–cooled isopentane for a few seconds. After thawing in 30% sucrose, corneas were washed in 0.1 M PB and then incubated in 0.01% hyaluronidase (type IV-S; Sigma-Aldrich, Inc, St Louis, MO) and 0.1% EDTA (Sigma) diluted in 0.1 M PB, pH = 5.3, at 37°C overnight in agitation. After washes in 0.1 M PB, corneas were incubated in 2.28% sodium metaperiodate ($NaIO_4$) for 5 minutes and in 0.05% sodium borohydride ($NaBH_4$) for 5 additional minutes. After further washes with PB, corneas were incubated in 10% normal goat serum in 0.1 M PB for 1 hour at 4°C to block nonspecific binding. Without washing, the corneas were subsequently incubated for 2 days at 4°C under agitation in mouse monoclonal primary antibody, neuronal class III beta-tubulin (anti-TUJ 1, catalog number MMS-435P; Covance Research Products, Berkeley, CA) at a concentration of 1:200 in 0.1 M PB plus 1% Triton X-100.[53]

2.1.3.1. Immunofluorescence

After further washes in PB, the tissue was transferred to Alexa 488 donkey anti-mouse (Molecular Probes; Invitrogen, Eugene, OR) diluted 1:100 in 0.1 M PB, 1% Triton X-100 for 1 day at 4°C. The corneas were finally washed in 0.1 M PB, included in mounting media (Citifluor; Citifluor Ltd, London, United Kingdom), and coverslipped for laser-scanning confocal microscopy viewing on a Leica TCS SP2 system (Leica Microsystems, Wetzlar, Germany). Immunohistochemical controls were performed by omission of either the primary or secondary antibodies.

2.1.3.2. Immunoperoxidase

After exposure to the primary antibody, the corneas were incubated for 1 day at 4°C in the secondary antibody biotinylated goat anti-mouse IgG (Jackson ImmunoResearch Laboratories, Inc, West Grove, PA) diluted 1:100 in 0.1 M PB + 1% Triton X-100. Corneas were rinsed again in PB and incubated for 1 day at 4°C in avidin–biotin–horseradish peroxidase complex (ABC reagent; Vector Laboratories, Burlingame, CA). Thereafter, they were incubated under agitation in the dark in 3,3′-diaminobenzidine tetrahydrochloride (DAB) (at 0.1% in 0.1 M PB) for 15 minutes and further incubated with fresh DAB solution with 0.01% H_2O_2.[53] The DAB reaction was stopped by washes in distilled water. The corneas were mounted in high adherence reagent-coated glass slides (Vectabond; Vector Laboratories, Burlingame, CA) and coverslipped. Light photomicrographs and camera lucida drawings were made in a Leica DMR microscope.

2.1.4. Electrophysiological recordings

Previous evidence[4] indicated that extracellular recording of nerve terminal impulse (NTI) discharges with a micropipette applied onto the corneal surface (Brock et al.,[14] 1998) favors the detection of the activity of cold receptor nerve terminals, whereas extracellular recording of single-parent nerve fibers dissected out of the ciliary nerves in the back of the eye predominantly selected polymodal and mechanonociceptor axons. Therefore, we alternated preparations of the isolated cornea, and of the excised whole eye with its sensory nerves, to record the impulse activity of the different functional types of peripheral corneal receptors. For this purpose, 1, 2, or 4 weeks after lachrymal gland removal, animals were killed with an intraperitoneal injection of 100 mg/kg sodium pentobarbitone and both eyes immediately enucleated together with the bulbar and tarsal conjunctiva and the optic and ciliary nerves, and placed in cold saline (4°C).

2.1.4.1. Recording of corneal mechanosensory and polymodal nociceptor fibers

Connective tissue and extraocular muscles were carefully removed from the excised eyeball to expose the back of the eye with the ciliary nerves around the optic nerve. The eye was then placed in a double chamber specially designed to keep the anterior segment of the eye with the conjunctiva, separated from the posterior segment and the ciliary nerves. In the front part of the chamber, the conjunctiva was pinned to the separating wall to isolate both compartments, which were perfused separately. The anterior compartment was perfused with warm saline (34°C) dropping continuously over the upper corneoscleral border. In the rear compartment of the chamber, filled with warmed mineral oil, nerve filaments were teased apart from the ciliary nerves and placed on an Ag–AgCl electrode for monopolar recording of single-unit impulse activity, using conventional electrophysiological equipment (gain ×10000, high-pass 300 Hz, low-pass 3 KHz; DAM50 amplifier; WPI, Sarasota, FL). Electrical signals were recorded with respect to an Ag/AgCl pellet in the posterior compartment. Electrical signals were transferred to a PC with a CED interface (CED micro1401 MK II; Cambridge Electronic Design, Cambridge, United Kingdom) and analyzed with appropriate software (Spike 2, v7.0, also from CED). Spontaneous activity of the selected unit was recorded during 1 minute before any intended stimulation. Mechanical threshold was determined thereafter using calibrated von Frey hairs (range 0.25-4.00 mN). Receptive fields of corneal afferent fibers were localized using mechanical stimulation with a fine paint brush and mapped afterwards using a suprathreshold von Frey hair. For chemical stimulation, a gas jet containing 98.5% CO_2 was applied on the corneal receptive field during 30 seconds. Thermal stimulation was performed by heating (up to 45°C) or cooling (down to 20°C) the perfusion solution by means of a custom-made Peltier device. In a group of experiments, the topical effect of menthol (100-200 μM) on polymodal nociceptor activity was also tested. For this purpose, a 6-mm piece of paper soaked in menthol was placed for 1 minute on the receptive field of the recorded polymodal nociceptor fiber. Response to mechanical and chemical stimulation performed before, immediately after application of the drug, and 15 minutes afterwards were compared.

2.1.4.2. Recording of corneal cold-sensitive nerve terminals

In this type of experiment, the corneas were cut circularly at the limbus with iris scissors, placed in a perfusion chamber, and secured with insect pins to the silicone bottom of the chamber (Sylgard 184; Dow Corning, Midland, MI). Corneas were continuously superfused at a flow of 2.5 mL/min with physiological solution (composition in millimolars: 133.4 NaCl; 4.7 KCl; 2 $CaCl_2$; 1.2 $MgCl_2$; 16.3 $NaHCO_3$; 1.3 NaH_2PO_4; and 7.8 glucose; gassed with carbogen: 95% O_2, 5% CO_2 to pH = 7.4). Temperature of the bath solution was maintained at 34°C (basal temperature) by means of a feedback-regulated, home-made Peltier device. The NTI activity of single-cold thermoreceptors terminals was recorded following the technique described by Brock et al.[14] (1998) using 50-μm diameter glass micropipette electrodes filled with bath saline solution, applied onto the surface of the cornea under slight suction. Electrical signals were recorded with respect to an Ag/AgCl pellet in the bath. Electrical activity was amplified (×1000, NL 103 AC amplifier; Digitimer, Welwyn, United Kingdom), filtered (high-pass 1 Hz, low-pass 5 KHz; NL 125/NL 126 filter, Digitimer) and stored in a computer, using a CED interface and Spike 2 software. Only NTIs originating from single cold-sensitive terminals were selected for further study. They were identified by their relatively high level of regular spontaneous discharge, occasionally in bursts, that increased prominently with cooling and silenced with warming of the superfusion solution.[4,5,14,15,24,60] Ongoing NTI activity at the basal mean temperature was recorded for at least 2 minutes before applying a cooling ramp to 15°C of 30-second duration, obtained by decreasing the temperature of the perfusion solution (average cooling rate −0.5°C per second). This was followed by rewarming to the baseline temperature. After a resting period of 2 minutes, corneal temperature was increased up to 50°C for 30 seconds to explore heat sensitivity (average heating rate +0.4°C). In a set of experiments, a stepwise cooling was performed from 34°C to 22°C in four −3°C steps of 2-minute duration. In another group of experiments, the effect of TRPM8 agonist menthol (50-200 μM) and tetrodotoxin-sensitive (TTX-s) Na^+ channel inhibitor hainantoxin-IV (100 nM)[78] on the spontaneous and evoked activity of cold receptors was tested. To study these effects, the corresponding drug was added to the physiological saline solution and perfused during 8 minutes; responses to thermal stimulation were tested before and during exposure to the drug.

2.1.4.3. Data analysis

In cold nerve terminal recordings, NTIs were discriminated during the acquisition process using a threshold criterion, and filtered manually afterwards to remove artifacts. Interval durations between successive NTIs (*interspike interval*) were first obtained. The following additional firing pattern parameters were calculated: *mean NTI frequency*: average number of NTIs recorded per second (impulses per second); *instantaneous frequency*: the

inverse of the time interval between successive NTIs, expressed in Hz; *cooling threshold*: temperature during the cooling ramp at which a 25% increase of the mean NTI frequency at basal temperature was obtained; *peak response*: maximal impulse per second value of NTI frequency during the cooling ramp; *temperature at the peak response*: temperature value (°C) at which peak frequency was reached. Also, to determine the effect of temperature on the shape of NTIs, the impulse duration and amplitude, and the mean rate of voltage change (dV/dt) during the upstroke and downstroke phases of the individual NTIs were measured.[60]

In single-fiber recordings of ciliary nerves, impulse firing of individual units discriminated accordingly to their stimulus modality, amplitude, and shape was analyzed. *Ongoing impulse activity* was expressed as mean impulse frequency (in impulses per second) measured during 30 seconds at the beginning of the recording and during the interstimulus periods. Responses to CO_2 were quantified measuring the following parameters: *latency*: time delay between onset of the CO_2 pulse and the first impulse given by the unit; *mean discharge rate*: mean number of impulses per second (imp/s) throughout the CO_2 pulse; *postdischarge*: mean firing frequency (imp/s) during 30-second immediately after the CO_2 pulse.[3,4]

2.1.5. Labelling of trigeminal ganglion corneal neurons

In guinea pigs anesthetized with 90 mg/kg ketamine and 5 mg/kg xylazine (i.p.), a 6 mm-diameter piece of Spongostan film (Ferrosan A/S, Soeborg, Denmark) saturated with the cell stain FM 1-43 (Molecular probes; Invitrogen) at 5 mM in saline solution was carefully placed in the center of the cornea to retrogradely label TG sensory cell bodies whose axons innervate the cornea. After 40 minutes, the film was removed and the eyes were repeatedly washed with warm (30°C) PBS.[74]

After 6 days, animals were killed with an overdose of sodium pentobarbital and both TGs were immediately removed and maintained in cold (4°C-5°C) Ca^{2+}- and Mg^{2+}-free Hanks balanced salt solution (HBSS) (Gibco) until dissociation of TG neurons for intracellular calcium imaging or electrophysiological recording.

2.1.6. Intracellular calcium imaging in trigeminal ganglion neurons

Trigeminal ganglia were incubated in a mixture of collagenase type XI (0.66 mg/mL) and dispase (3 mg/mL) for 1 hour followed by mechanical dissociation. The cell suspension was then layered on top of a 14% Percoll (Sigma) gradient to separate myelin and nerve debris from the neurons. Next, the cell suspension was centrifuged at 2500 rpm for 13 minutes at room temperature. Neurons found in the pellet were suspended in 3 mL HBSS + 10% fetal bovine serum (Invitrogen), centrifuged at 1500 rpm for 5 minutes and resuspended in the culture medium (89% Minimum Essential Media and 10% fetal bovine serum supplemented with 1% Minimum Essential Media vitamins [all from Invitrogen], plus 100 μg/mL penicillin/streptomycin, and 100 ng/mL nerve growth factor [all from Sigma]). Cell suspensions were transferred to poly-L-lysine/laminin-coated 6 mm-diameter glass coverslips and incubated at 37°C up to 1 day.[52] Corneal neurons labeled with FM 1-43 were identified by their fluorescence emission when excited with 470-nm light. Each coverslip contained only one or 2 labeled neurons, where intracellular calcium or ion currents were subsequently measured.

Changes in intracellular calcium levels were measured using ratiometric digital fluorescence calcium imaging. Neurons were incubated with 5 μM Fura-2 AM (Invitrogen) for 1 hour at 37°C in the dark.[52] Then, the coverslip was placed into a small chamber continuously perfused at 3 mL/min with (in millimolars) 140 NaCl, 3 KCl, 2.4 $CaCl_2$, 1.3 $MgCl_2$, 10 HEPES, and 10 glucose, at pH = 7.4 adjusted with NaOH. The temperature of the perfusion solution was maintained at 34°C (basal temperature) or decreased to 15°C for 30 seconds (cooling ramp stimulus) using a feedback-controlled home-made Peltier device. Then, 100 μM menthol, 100 μM cinnamaldehyde, and 1 μM capsaicin (all from Sigma) were added to the perfusion solution for 3 minutes to test the effects of TRP channel agonists. The response to 30 mM KCl was explored at the end of each experiment and those neurons not producing a $[Ca^{2+}]_i$ increase in response to this depolarizing stimulus were discarded. Fluorescence measurements were made with a Zeiss Axioskop FS upright microscope fitted with an ORCA-ERCCD camera (Hamamatsu Photonics). Fura-2 was excited at 340 and 380 nm (excitation time 300 milliseconds) with a rapid switching monochromator (TILL Photonics GmbH, Graefelfing, Germany), and the emitted fluorescence was filtered with a 510-nm long-pass filter. Mean fluorescence intensity ratios (F_{340}/F_{380}) were displayed online with MetaFluor software (Molecular Devices, Sunnyvale, CA). Fluorescence signals and bath temperature were recorded simultaneously.

The following parameters were measured in FM 1-43-labeled TG neurons from both control and tear-deficient guinea pigs: *peak response* to cold, defined as the peak value of the F_{340}/F_{380} ratio during the cooling ramp. *Temperature at the peak of the response*, defined as the temperature at which the positive peak of the first derivative of the fluorescence ratio was obtained. *Cold threshold*, ie, the temperature decrease required to evoke a $[Ca^{2+}]_i$ response, determined and expressed as the temperature change at which the F_{340}/F_{380} rose 4 SD over its basal value at 34°C.

2.1.7. Patch-clamp recording of trigeminal ganglion neurons

Trigeminal ganglion cell suspensions were transferred to poly-L-lysine/laminin–coated 12-mm-diameter glass coverslips and incubated at 37°C up to 1 day. FM 1-43-labeled neurons from control and tear-deficient animals (1-2 by coverslip) were identified and used for patch-clamp electrophysiological recordings.

2.1.7.1. Cold-evoked currents

Coverslips with cultured cells were placed in a microchamber and continuously perfused (0.8 mL/min) with solutions warmed at 33 ± 1°C. The temperature was adjusted with a water-cooled Peltier device (RDTC-1, Reid-Dan Electronics) placed directly on the cell field and controlled by a feedback device.[75] Cold sensitivity was investigated with a temperature ramp to 15°C performed during perfusion with the standard bath solution or containing 100 μM menthol.

Cold-evoked currents in FM 1-43-labeled TG neurons were monitored at −60 mV in the whole-cell patch clamp configuration, filtered at 2 kHz and sampled at 10 kHz. Current recordings were performed simultaneously with temperature recordings.[52] The standard bath solution contained the following (in millimolars): 140 NaCl, 3 KCl, 1.3 $MgCl_2$, 2.4 $CaCl_2$, 10 HEPES, and 10 glucose, pH = 7.4 adjusted with NaOH (297 mOsm/kg). Standard patch pipettes 5 to 8 MΩ were fabricated from borosilicate glass capillaries (Harvard Apparatus, Edenbridge, Kent, United Kingdom) and contained the following (in millimolars): 140 KCl, 6 NaCl, 1 EGTA, 0.6 $MgCl_2$, 1 NaATP, 0.1 NaGTP, and 10 HEPES, at pH = 7.4 adjusted with KOH (282 mOsm/kg).

Current signals were recorded with an Axopatch 200B amplifier (Molecular Devices, Sunnyvale, CA). Stimulus delivery and data acquisition were performed using pClamp 9 software (Molecular Devices). Analysis was performed with pClamp 9 and WinASCD software (Guy Droogmans, Katholieke Universiteit Leuven, Leuven, Belgium).

2.1.7.2. Na^+ and K^+ currents

An Axopatch 200B amplifier (Molecular Devices, Union City, CA) was used for patch-clamp recordings of FM 1-43-labeled neurons. Membrane currents were recorded in the whole-cell patch clamp configuration, filtered at 2 kHz, digitized at 10 kHz, and acquired with pClamp 9 software (Molecular Devices). Recordings were analyzed with Clampfit 9 (Molecular Devices) and Prism 4 (GraphPad Software, Inc, La Jolla, CA). Whole-cell capacitance and series resistance were compensated with the amplifier circuitry. Series resistance was always kept below 10 MΩ and compensated at 70% to 80%. All recordings were done at room temperature (23°C). Patch electrodes were fabricated in a Flaming/Brown micropipette puller P-97 (Sutter Instruments). Electrodes had a resistance between 2 and 3 MΩ when filled with intracellular solutions.

To record Na^+ currents, the following solutions were used: intracellular solution contained (in millimolars) 100 Cs^+-methanesulfonate, 40 tetraethylammonium chloride, 5 Na Cl, 1 $CaCl_2$, 2 $MgCl_2$, 2 ATP, 1 GTP, 11 EGTA, and 10 HEPES at pH = 7.2 (310 mOsm/kg). Extracellular solution contained (in millimolars) 35 NaCl, 65 choline-Cl, 30 tetraethylammonium chloride, 0.1 $CaCl_2$, 5 $MgCl_2$, 10 HEPES, and 10 glucose at pH = 7.4 (325 mOsm/kg). As previously described,[30,31] from a holding voltage of −80 mV, voltage-gated Na^+ currents were evoked after a 500-millisecond voltage step to either −120 or −40 mV. Current evoked from −40 mV was considered to be TTX-resistant (TTX-r) current, whereas the difference between the current evoked from −120 and −40 mV was considered to be TTX-s I_{Na}. Currents were evoked after a 500-millisecond prepulse to either −120 or −40 mV with a 100-millisecond step to potentials between −60 and +50 mV in 10 mV increments. After recording Na^+ currents, neurons were challenged with 100 μM menthol, 100 μM allyl isothiocyanate (AITC), and 1 μM capsaicin. Inward currents activated by these compounds were used to classify neurons as cold sensory neurons or polymodal nociceptor neurons.

The voltage dependence for activation of I_{Na} was determined from the peak sodium conductance (g_{Na}) at different potentials, calculated as a chord conductance, from the corresponding peak current, as $g_{Na} = I_{Na}/(V_m - E_{Na})$, where E_{Na} is the reversal potential for sodium current. E_{Na} was determined for each neuron wherein the current values around the reversal potential were fit with a linear regression line to determine the voltage at which the current was zero. The conductance values were fitted to a Boltzman function using a least-squares fit to characterize the activation characteristics $G/G_{max} = 1/\{1 + \exp([V_{0.5} - V_m]/k)\}$, where $V_{0.5}$ is the voltage for half-maximum activation and k is the slope factor.

To record K^+ currents, the intracellular solution used was (in millimolars): 120 K^+-gluconate, 20 KCl, 2 $MgCl_2$, 1 $CaCl_2$, 10 HEPES, 10 EGTA, and 1 mM ATP at pH = 7.2. Extracellular solution contained (in millimolars): 150 choline-Cl, 5 KCl, 2 $CaCl_2$, 1 $MgCl_2$, 10 HEPES, 0.2 $CdCl_2$, 5 glucose, and 1 μM TTX at pH = 7.4. Solutions were adjusted to 310 mOsm/kg with sorbitol. K^+ currents were separated into 3 groups based on inactivation properties: rapidly inactivating, slowly inactivating, and non-inactivating currents, that presumably correspond to the previously described rapidly inactivating ($K_{A,fast}$) and slowly inactivating ($K_{A,slow}$) A-currents and delayed rectifier current (K_{dr}), respectively.[29,54] Protocol 1 consisted of voltage-clamp steps (−100 to +50 mV; 500 milliseconds) made from a holding potential of −100 mV and activating a family of mixed outward current components.[49] Protocol 2 was similar to protocol 1 but included a short depolarizing prepulse to −10 mV (60 milliseconds) that preferentially removed a rapidly inactivating component, leaving more slowly and noninactivating components. The rapidly inactivating component was isolated by subtracting the traces generated with protocol 2 from those generated with protocol 1. Protocol 3 was similar to protocol 1 but cells were held at −10 mV (instead of −100 mV) for 7 seconds, which inactivated both the rapidly and slowly inactivating currents and test steps resulted in traces consisting of the noninactivating component and leak current. The leak current was subsequently subtracted out with a p/8 leak subtraction protocol, isolating the noninactivating current. The slowly inactivating component was isolated by subtracting currents generated with protocol 3 from the ones generated with protocol 2. Similarly to Na^+ currents, activation voltage dependency was studied by plotting normalized conductance (G/G_{max}) against test pulse voltage and fitting the data using a Boltzmann function. To study the voltage dependency of inactivation for $K_{A,fast}$ and $K_{A,slow}$ 2-pulse voltage protocols were used. Residual $K_{A,fast}$ currents were measured following short (1 second) conditioning prepulse varying between −120 and 0 mV, followed by a 400-millisecond test pulse of +50 mV, which allowed inactivation of only the rapidly inactivating $K_{A,fast}$ currents. Longer conditioning pulses (8-second duration; −80 to 0 mV) allowed inactivation of both $K_{A,fast}$ and $K_{A,slow}$ currents. Current amplitude measured at the test pulse was plotted against conditioning pulse potential, and the continuous line is an average of fits to a negative Boltzmann function: $I/I_{max} = 1/(1 + \exp[V_{0.5} - V_m/k])$, where I is the current, I_{max} is the maximal current, $V_{0.5}$ is the membrane potential for half-activation, V_m is the command potential, and k is the slope factor.

2.2. Human experiments

Eighteen healthy subjects (14 females and 4 males, mean age 33.3 ± 2.3 years, range 20-54) and 9 patients with dry eye (7 female, 2 male; mean age 43.5 ± 5.4 years, range 25-70) were recruited and participated voluntarily in the study. Patients with moderate DED were selected according to the following inclusion criteria: Ocular Surface Disease Index >15 and <40, Schirmer test <10 mm in 5 minutes, tear break-up time test ≤10 seconds, absence of ocular pathologies different from DED, and absence of systemic diseases. All the participants signed informed consent to a protocol approved by the Ethical Review Committees of the University Miguel Hernandez and the Hospital Universitario Central de Asturias that followed the tenets of the Declaration of Helsinki and the Spanish and European Union regulations. An abbreviated medical history was obtained from all the subjects and patients, including age, sex, and time from dry eye diagnosis. Contact lens wearers and subjects who had previously undergone ocular surgery were not included in the study. Before testing, the ocular surface of each patient was examined by biomicroscopy to ascertain the absence of any ocular pathology other than aqueous tear-deficient DED.

2.2.1. Experimental protocol

The volunteers seated comfortably upright under constant temperature (23°C) and humidity conditions (60% humidity), looking to a white wall. Illumination of the room was also constant.

A high sensitivity webcam was placed above the visual axis of the subject, at a distance of 1 m, for continuous video recording. The participant was aware of the camera but unaware of its use for off-line counting of blinks. At the beginning of the session, the volunteers were filmed at rest for 3 minutes to determine the basal blink rate. Then, participants were asked to fill in the Ocular Surface Disease Index questionnaire validated for Spanish speakers,[25] and to evaluate the sensation of eye discomfort using a visual analog scale (VAS) from 0 (no discomfort) to 100 (the maximum discomfort they can imagine). Tear osmolarity was then measured using a lab-on-a-chip system that collects a 50-nL tear sample from the temporal side of the inferior lid margin and analyses its electrical impedance to calculate the concentration of ions within the tear fluid (TearLab Corp, San Diego, CA). The Schirmer test without anesthesia was performed 10 minutes afterwards using commercial paper strips of known water absorption quality (Dina Strip Schirmer-Plus, Gecis, Lamotte, France). The lower lid margin was slightly pulled down and the paper strip was folded along the printed bold line and was gently placed over the lower temporal lid margin. The eye remained closed for 5 minutes, and the paper strip was gently removed afterwards. The length of the wet portion of the paper strip was then measured from the bold printed line, and the tearing rate was expressed as the length of wet paper per 5 minutes (mm per 5 minutes).

After a 10-minute rest period, a sterile soft paraffin ointment containing menthol at 1 mM was applied to the malar region of the skin, at a distance of 2.5 cm from the lower lid margin to avoid direct spread of menthol or lipids into the tears,[73] using a cotton swab. After 3 minutes, the volunteers rated the magnitude of cooling and unpleasant components of the sensation experienced at the ocular surface produced by menthol, using 2 separate 10-cm continuous VASs. The subjects were also asked to describe in their own words the sensation experienced in the eye after ointment application. A sample of tear was taken thereafter, approximately 4 minutes after ointment application. The Schirmer test and tear break-up time test determination were performed after 3 minutes. After a 10-minute resting period, the procedure was repeated using an ointment containing 10 mM menthol. Menthol sterile ointments were prepared at the Instituto Oftalmológico Fernandez-Vega facilities. In a set of experiments, the same experimental protocol was repeated in volunteers subjected to a continuous air jet (velocity: 6.5-7.5 m/s, ie, 24-27 km/h, equivalent to staying under a moderate breeze or cycling under no wind) at room temperature directed to both eyes. The cross-sectional area of the airstream was 250 cm^2.

Menthol concentration in tear samples was quantified using gas chromatography with a flame ionization detector. Tears collected with a glass capillary 5 minutes after ointment application to the malar skin and frozen until measurement were used to determine menthol concentration in tears using a gas chromatograph (CLARUS 400, PerkinElmer, Inc, Shelton, CT) provided with an Elite-Wax column (30 m × 0.32 mm i.d. × 0.5 μm df; also from PerkinElmer). Helium was used as the carrier gas and camphor as internal standard. The initial column temperature was 100°C, increasing at 30°C/min to 200°C (hold 2 minutes). The injector temperature was 200°C, and the interface temperature was 240°C.

2.3. Statistical analysis of data

Statistical comparisons were made using Statistica 6.0 (StatSoft Inc, Tulsa, Ok), SigmaStat 3.5 (Systat Software, Erkrath, Germany), and Prism 4 (GraphPad Software, Inc) data analysis software. SigmaStat was used to determine the normality, sample size, and sensitivity of the experimental designs. Previous analysis of the sample size and test power was required by the Ethics Committee of the University Miguel Hernández to approve the use of animals in research. Data were expressed as mean ± SEM, and n the number of nerve terminals, fibers, neurons, corneas, or subjects explored. Data were compared using parametric or their equivalent nonparametric tests, as indicated. Analysis of variance (ANOVA) with the post hoc Dunnett test or repeated-measures ANOVA were used as indicated. In the case of multiple comparisons, for instance over a voltage range, data were initially analyzed using an ANOVA with repeated measures. If this revealed a significant difference, Student *t* tests were applied for post hoc testing with a Bonferroni correction. The Z test was used to compare proportions. The significance level was set at $P < 0.05$ in all statistical analyses.

3. Results

3.1. Tearing, blinking, and corneal nerve morphology are altered in guinea pig tear-deficient eyes

Mild conjunctival hyperemia was observed 1 and 4 weeks after surgical removal of the exorbital lachrymal gland in all experimental animals. Occasional mild punctate staining but no epithelial defects were detected in the cornea with fluorescein staining at any time point after surgery. At the end of the first postoperative week, we confirmed a significant reduction in tear secretion volume to 30% of the baseline value, and this remained low until the last measurement taken 1 month after the intervention ($P < 0.001$, repeated-measures 1-way ANOVA; **Fig. 1A**). Intriguingly, the tearing rate in the contralateral eye was also significantly reduced 4 weeks after surgery ($P = 0.018$, paired *t* test), albeit less than in the operated side (**Fig. 1B**). Blinking frequency in both eyes was slightly higher than in the controls 1 week after surgery (2.4 ± 0.6 vs 1.6 ± 0.3 blinks per minute: $P = 0.208$, paired *t* test), although this parameter returned to basal values 2 and 4 weeks after surgery.

We took advantage of this model to explore whether the chronic tearing deficit and the prolonged ocular surface dryness provoked in these corneas altered the morphology, distribution, and density of the sensory afferent nerve fibers stained with a monoclonal antibody against neuronal class III beta-tubulin (TuJ1).[53] TuJ1-positive nerve fibers were distributed homogeneously throughout the surface of corneas from control, nonoperated animals (n = 3; **Fig. 2A**). Typically, stromal nerve bundles sent perpendicular, ascending branches that traversed the Bowman membrane and divided into several, parallel long subbasal nerve fibers (leashes) within the basal epithelium cell layer (**Fig. 2B**). Branches from these leashes ascended perpendicularly towards the outermost corneal epithelium layers, where they ended as asymmetric clusters of free nerve terminals (**Fig. 2C**).[39,53,60] By contrast, there were significantly fewer peripheral subbasal leashes throughout the cornea 4 weeks after removal of the lachrymal gland, these leashes presenting a quite tortuous trajectory that covered shorter distances (**Figs. 2D and E**). Moreover, the terminal ramifications of the branches arising from the leashes were less abundant, and they had a distinct morphology in these corneas, which had significantly fewer nerve terminals (**Figs. 2F–I**).

3.2. Corneal cold sensory nerve fibers exhibit abnormal activity after prolonged eye dryness

Having seen that the dryness produced by removing the lachrymal gland affected nerve architecture in the cornea, we assessed whether the responsiveness of the different functional types of sensory receptors innervating the corneal surface to natural stimuli was also altered. For this purpose, we recorded the impulse activity

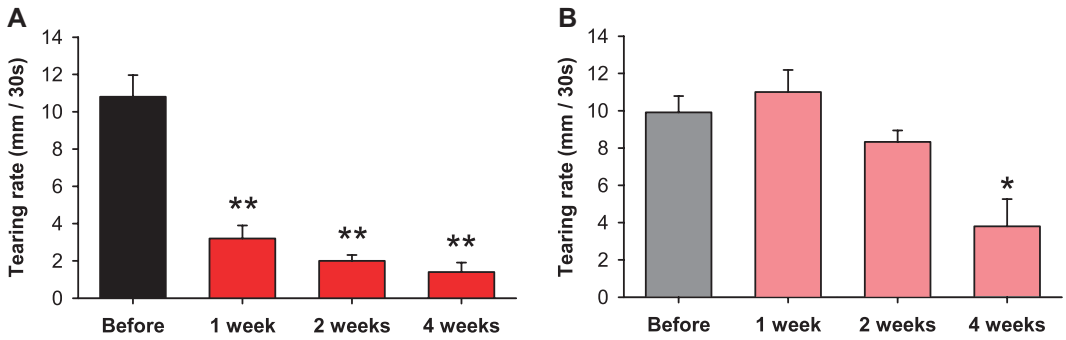

Figure 1. Tearing rate determined at different time points (1-4 weeks) after unilateral removal of the main lachrymal gland in the guinea pig. Basal tearing rate expressed as the mean wetted length (in millimeters) of the phenol red thread placed in the lower lid for 30 seconds was measured in the same animals (n = 5) before and at different time points after surgery, (A) in the operated side and (B) in the contralateral eye. $^{**}P < 0.001$, 1-way repeated-measures analysis of variance with the post hoc Dunnett test. $^{*}P < 0.05$, paired *t* test, difference from the tearing rate before surgery.

of single afferent fibers dissected from the ciliary nerves of excised and superfused guinea pig eyes from control and operated animals, 1 to 4 weeks after lachrymal gland removal. In the intact cornea, sensory afferents identified as mechanosensory and polymodal nociceptor fibers[9,10,24] presented corneal receptive fields usually extending up to 1 mm into the adjacent sclera and were in most cases silent at rest, both responding to mechanical stimulation and in the case of polymodal nociceptors also to 98.5% CO_2 jets (**Fig. 3A**; the functional characteristics of both these types of sensory afferents are summarized in **Table 1**).

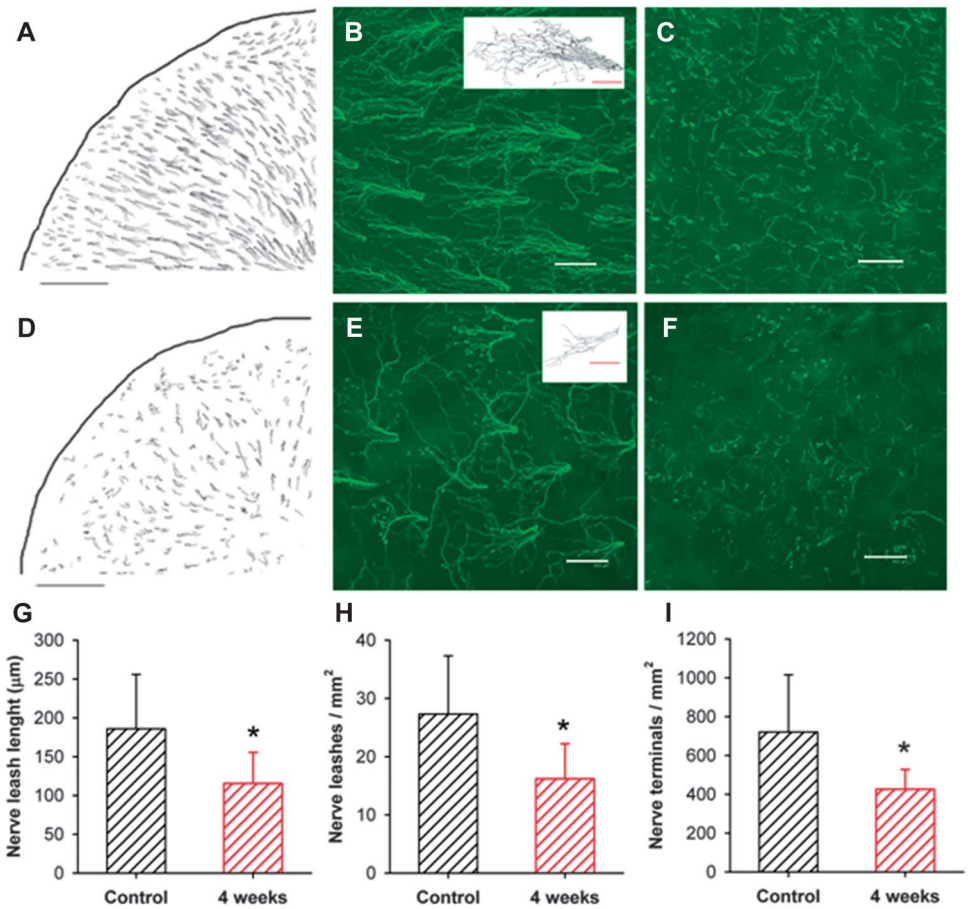

Figure 2. Morphological changes of corneal nerves at 4 weeks after removal of the main lachrymal gland (tear-deficient corneas). (A) Camera lucida drawing of the subbasal plexus from a quadrant of a control cornea. (B) Tuj-1-positive subbasal nerves (leashes) in a control cornea. Inset: drawing of a subbasal nerve ramification (leash). (C) Epithelial nerve endings in a control cornea labeled with Tuj-1. (D) Camera lucida drawing of subbasal plexus from a quadrant of a tear-deficient cornea. (E) Tuj-1-positive subbasal nerves in a tear-deficient cornea. Inset: drawing of a subbasal nerve ramification. (F) Tuj-1-positive epithelial nerve endings in a tear-deficient cornea. (G) Average length of subbasal nerve leashes in control and tear-deficient corneas. (H) Average density of corneal subbasal nerve leashes per squared millimeter in control and tear-deficient corneas. (I) Average density of nerve terminals per squared millimeter in control and tear-deficient corneas. Data shown in (G–I) are mean ± SEM of data from 4 control and 8 tear-deficient animals; $^{*}P < 0.05$, *t* test. Scale bars: A, D = 1000 μm; B, C, E, F = 100 μm; inset = 40 μm.

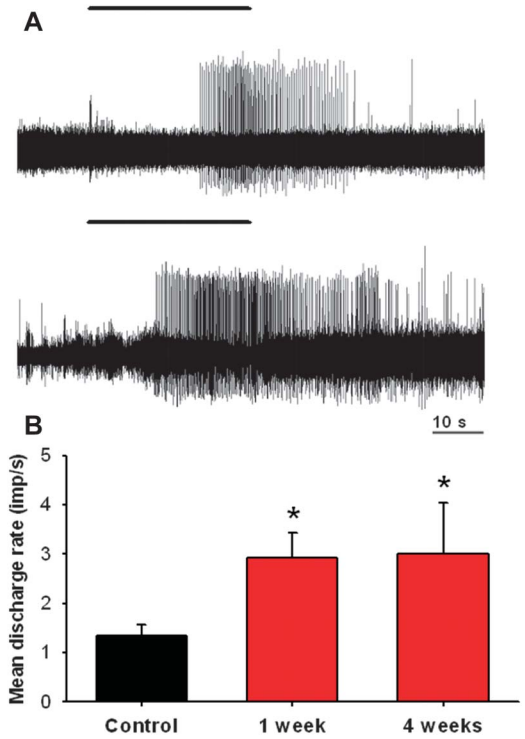

Figure 3. Chemical sensitivity of polymodal nociceptor nerve fibers recorded from control and tear-deficient corneas 4 weeks after lachrymal gland removal. (A) Sample recording of the response of corneal polymodal nociceptor fibers to chemical stimulation of the receptive field with a 30-second-duration CO_2 pulse in control (upper trace) and tear-deficient corneas (lower trace). The bars indicate the duration of the stimulus. Notice that the impulse discharge evoked by CO_2 overpassed in both cases the duration of the stimulus (postdischarge). (B) Mean discharge rate of polymodal nociceptor fibers during the CO_2 pulse in control (n = 18) and tear-deficient corneas (1 week, n = 25; 4 weeks, n = 8). Data are mean ± SEM; $P < 0.001$, 1-way analysis of variance with the Dunnett test (*$P < 0.05$).

One week after lachrymal gland removal, the mechanical thresholds of mechanonociceptors and polymodal nociceptors remained unaltered. However, more fibers displayed ongoing activity at rest than in control eyes, both among mechanonociceptor (38% vs 7%; $P < 0.05$, Z-test) and polymodal nociceptor fibers (33% vs 9%; $P < 0.05$, Z-test). Moreover, mean ongoing firing frequency of the spontaneously active fibers was significantly higher in mechanonociceptors (**Table 1**). We also noticed that a fraction of the polymodal fibers in tear-deficient eyes readily developed ongoing activity after applying the initial CO_2 pulse used to search for chemical sensitivity (**Table 2**), and in some of them spontaneous paroxysmal discharges occasionally occurred. In addition, 1 week after surgery, the mean discharge rate evoked by CO_2 pulses in polymodal nociceptors of tear-deficient corneas was larger ($P < 0.05$) and the latency in the onset of this impulse response was shorter ($P < 0.001$). By contrast, the mean discharge rate of the postdischarge after chemical stimulation was only slightly but not significantly increased ($P = 0.113$; **Table 2**). Altogether, these changes seem to reflect the development of a moderate degree of corneal polymodal nociceptor sensitization[9,10,24] in the days after lachrymal gland excision. Four weeks after surgery, the proportion of spontaneously active mechanonociceptor and polymodal nociceptor fibers had returned to normal levels (**Table 1**). The only functional difference between both classes of afferents in control corneas and in corneas exposed to reduced tearing for 4 weeks was that polymodal nociceptor fibers maintained an augmented firing response to CO_2, which additionally started at a significantly shorter latency (**Figs. 3A and B** and **Table 2**).

We also recorded the impulse activity at nerve terminals of cold thermoreceptor fibers, which represent approximately 10% of all corneal sensory afferents, confirming in intact eyes their regular ongoing impulse activity at 34°C and the marked increase in frequency caused by 15°C cooling pulses (**Fig. 4A**), characteristic of ocular cold thermoreceptors.[14,15,24,60] Notably, corneal cold endings in eyes deprived of the lachrymal gland developed progressively, in the weeks after surgery an increase in the ongoing firing frequency at the basal temperature of 34°C, as well as comparatively larger responses to cooling pulses (**Fig. 4B**).

The various parameters that define cold receptor activity at these endings were assessed in control corneas and in corneas 4 weeks after removal of the lachrymal gland, and are summarized in **Table 3**. **Figure 4C** represents the mean firing frequency in response to a cooling ramp in both conditions. As soon as 1 week after surgery, the cooling threshold had already moved to warmer values (**Fig. 4D**). Ongoing NTIs frequency at 34°C also rose gradually in tear-deficient eyes, becoming significantly higher in comparison with control corneas 4 weeks afterwards (**Fig. 4E**). The same was true for the peak firing frequency evoked by cooling ramps (**Fig. 4F**). Moreover, such higher peak frequency values were attained at temperatures of around 29°C, a warmer value in comparison with intact animals (**Table 3**). The differences in excitability and responsiveness between corneal cold nerve terminals of intact and tear-deficient eyes were also evidenced in the interval distribution histograms of cold nerve impulse activity. In corneas with a reduced tear flow, the intervals between NTIs fired at the temperature at which the peak frequency discharge

Table 1

General properties of mechanonociceptor and polymodal nociceptor fibers recorded in control corneas, and 1 and 4 weeks after surgical removal of the lachrymal gland.

	Control	Time after lachrymal gland removal	
		1 wk	4 wk
Mechanonociceptor fibers	n = 55	n = 17	n = 12
Receptive field diameter (mm)	3.85 ± 0.08	3.19 ± 0.17	2.70 ± 0.26
Spontaneous activity (imp/s)	0.02 ± 0.02 (4/55)	0.30 ± 0.22* (6/16)	0.00 ± 0.00 (0/12)
Mechanical threshold (mN)	0.89 ± 0.13	0.52 ± 0.11	0.61 ± 0.15
Polymodal nociceptor fibers	n = 34	n = 27	n = 8
Receptive field diameter (mm)	3.65 ± 0.12	3.19 ± 0.17	2.88 ± 0.30
Spontaneous activity (imp/s)	0.09 ± 0.09 (3/34)	0.36 ± 0.31 (9/27)	0.00 ± 0.00 (0/8)
Mechanical threshold (mN)	0.32 ± 0.02	0.45 ± 0.10	0.29 ± 0.0

Data are mean ± SEM; n = number of fibers; numbers in brackets indicate the number of fibers with spontaneous activity/number of recorded fibers.
* $P < 0.05$, *t* test, difference from the control.

Table 2

Characteristics of the response to CO_2 of corneal polymodal nociceptors, recorded in control corneas, and 1 and 4 weeks after removal of the lachrymal gland.

	Control (n = 18)	Time after lachrymal gland removal	
		1 wk (n = 25)	4 wk (n = 8)
Ongoing activity (imp/s)	0.07 ± 0.07	0.23 ± 0.06*	0.06 ± 0.01
Latency (s)	18.3 ± 1.8	9.4 ± 1.6*	9.8 ± 3.9†
Mean discharge rate (imp/s)	1.34 ± 0.23	2.93 ± 0.50†	3.01 ± 1.02†
Postdischarge (imp/s)	0.81 ± 0.19	3.17 ± 0.86	1.40 ± 0.38

Data are mean ± SEM; n = number of fibers.
* $P < 0.001$, 1-way analysis of variance with the Dunnett test for differences from the control.
† $P < 0.05$, 1-way analysis of variance with the Dunnett test for differences from the control.

was attained, were shorter and of more uniform duration than those of control animals, reflecting the higher firing frequency attained during the cooling ramps in tear-deficient corneas (**Figs. 4C and G**).

We further analyzed in control and 4-week tear-deficient corneas the changes in cold thermoreceptor impulse activity evoked by a stepwise cooling between 34°C and 22°C in steps of −3°C (**Figs. 4H and I**). The static discharge frequency tended to be higher and the peak frequency of the dynamic response was smaller for temperature values over 26°C in tear-deficient eyes, which reflects that cold thermoreceptors fired at a higher frequency at any static temperature but were less able to encode dynamic temperature reductions (**Figs. 4H and I**). Finally, at low static temperatures, the NTIs in the tear-deficient corneas were significantly wider and had smaller amplitude (**Figure 5**). The different amplitude and shape of NTIs of cold nerve terminals are due to changes in local generator currents[14,15] being consistent with an alteration in the expression of ion channels involved in the stimulus transduction, and/or the generation of propagated nerve impulses.

3.3. Membrane currents of corneal cold TG sensory neurons are disturbed in tear-deficient animals

Transduction of temperature reductions by corneal cold thermoreceptors is mainly mediated by TRPM8 channels.[18,55,61] Thus, we used cultured adult corneal TG neurons retrogradely labeled with FM1-43 obtained from control guinea pigs (n = 14) and from animals in which the lachrymal gland was removed 4 weeks earlier (n = 18: **Fig. 6A**), to compare changes in somal intracellular calcium levels ($[Ca^{2+}]_i$) evoked by both thermal (a cooling ramp from 35°C to 15°C) and chemical stimuli (1 μM capsaicin, 100 μM cinnamaldehyde, and 100 μM menthol). Putative cold thermosensitive neurons were identified by their positive response to cold and 100 μM menthol[75] (**Figs. 6B and C**, blue traces), whereas neurons insensitive to cold stimuli but activated by cinnamaldehyde and/or capsaicin were classified as corneal polymodal nociceptor neurons (**Figs. 6D and E**, blue traces).

We did not detect significant differences in the $[Ca^{2+}]_i$ response to 100 μM menthol or to a cooling ramp between corneal cold-sensitive neurons from control (n = 36) and from tear-deficient animals (n = 29) (**Figs. 6F and G**) or in the amplitude of the I_{cold} current monitored at −60 mV (−80 pA, n = 7 vs −114 pA, n = 9, medians of control and tear-deficient, respectively; $P = 0.916$, Mann–Whitney rank-sum test), the $I_{menthol}$ current (−62 pA, n = 8 vs −69 pA, n = 7; $P = 0.878$, Mann–Whitney test) or the $I_{menthol + cold}$ current (−409 pA, n = 7 vs −642 pA, n = 6; $P = 1.0$, Mann–Whitney test). Likewise, the $[Ca^{2+}]_i$ response to cinnamaldehyde and capsaicin was of a similar amplitude in putative polymodal neurons from both groups of animals (9 and 15 neurons, respectively, data not shown). Taken together, these data suggest that cold-evoked currents that are largely mediated by TRPM8 channels in corneal thermoreceptor TG neurons[60] were not markedly altered in tear-deficient eyes.

The changes in excitability observed in corneal cold terminals exposed to reduced ocular surface wetness are suggestive of alterations in sodium currents (I_{Na}), similar to those that take place after injury of peripheral sensory nerves.[2,69] To explore this possibility, we recorded the TTX-r and TTX-s I_{Na} in retrogradely labeled corneal TG neurons from intact (n = 8) and operated guinea pigs (n = 8) (**Fig. 7A**). Based on their positive response to 100 μM menthol and their insensitivity to 1 μM capsaicin and 100 μM AITC, 7 of 25 neurons from control animals and 7 of 26 from operated animals were classified as cold-sensitive. Despite the apparently higher current density in neurons of tear-deficient animals, TTX-r current was not significantly different from control guinea pigs ($P = 0.16$, *t* test). However, conductance–voltage relationship for TTX-r I_{Na} activation in neurons of operated eyes seemed to have shifted significantly towards more negative voltages without modification in the slope factor (**Figs. 7B and C** and **Table 4**). Interestingly, TTX-s I_{Na} current amplitude in cold-sensitive corneal neurons was significantly larger at −40 and −30 mV in neurons from the operated animals (**Fig. 7D**). The mid point of activation was significantly shifted towards more hyperpolarized voltages in tear-deficient animals (**Fig. 7E**), which implies that TTX-s I_{Na} was activated at more negative membrane potentials. No significant differences were observed between the slope factors of the activation curves (**Table 4**).

From these data, we concluded that the disturbed sodium currents found in the soma of corneal cold neurons of operated animals could be one of the causes of the increased excitability of peripheral terminations in these neurons in tear-deficient eyes. Indeed, hainantoxin-IV, a neurotoxin that selectively inhibits TTX-s Na^+ channels[78] did reduce at 100 nM the spontaneous and cold-evoked activity of cold nerve terminals from both tear-deficient and control corneas (**Fig. 8**), which supports the hypothesis that TTX-s currents are stronger in corneal nerve terminals subjected to chronic dryness, thereby contributing to their enhanced excitability.

Increased Na^+ currents appearing in primary sensory neurons after peripheral injury or inflammation are often accompanied by dampened K^+ currents.[1,67] We examined the calcium-independent K^+ currents in corneal cold sensory neurons from control and tear-deficient animals (n = 7 and 8, respectively). Rapidly inactivating ($K_{A,fast}$) and slowly inactivating ($K_{A,slow}$) K^+ currents were significantly weaker in corneal cold neurons of tear-deficient eyes than in those of control eyes, and current–voltage relationships were significantly different for both currents (**Figs. 9A and B** and **Table 5**), whereas the noninactivating K^+ currents (K_{dr}, delayed rectifier) were similar in both groups (**Fig. 9C**). The activation and voltage dependency of the 3 kinetically separate current components were not significantly different between the control and tear-deficient eyes. By contrast, a significant difference was observed between corneal cold neurons of control and tear-deficient eyes in terms of the voltage-dependence of inactivation for $K_{A,fast}$ but not for $K_{A,slow}$ (**Table 5** and **Fig. 10**).

Collectively, our electrophysiological analysis of corneal cold neurons from intact and tear-deficient animals revealed that the enhancement of sodium currents was accompanied by an impairment of K^+ currents in animals with dry eye, in particular the rapidly and slowly inactivating K^+ currents whereas cold-activated current remained essentially unaffected. These disturbances are likely to at least partially underlie the enhanced excitability exhibited by corneal cold sensory fibers in tear-deficient eyes.

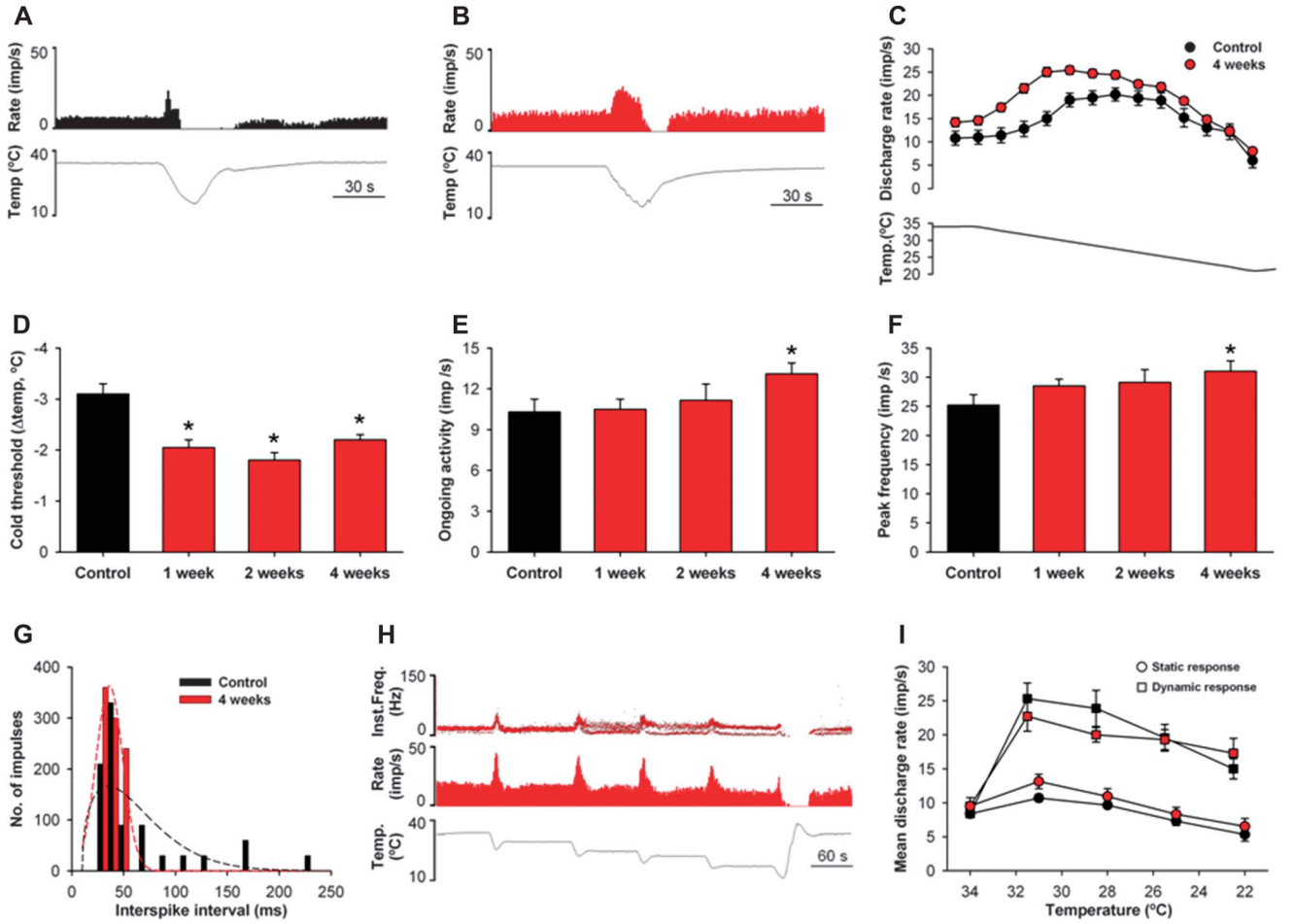

Figure 4. Responses to cooling of cold-sensitive nerve terminals in control and tear-deficient animals. (A) Sample recording of a single cold-sensitive nerve terminal recorded from a control cornea. Upper channel: Nerve terminal impulse (NTI) firing rate (imp/s); lower channel: temperature values (°C) of the perfusion solution along the record. (B) Sample recording of a single cold sensitive nerve terminal from a tear-deficient cornea, at 4 weeks after lachrymal gland removal. (C) Response of cold nerve terminals from control (n = 45) and tear-deficient corneas (n = 57) to a cooling ramp from 34°C to 21°C. Data are mean ± SEM of the mean discharge rate at the corresponding temperatures of the ramp. Repeated-measures analysis of variance (ANOVA), $P < 0.005$; post hoc comparison using the *t* test with Bonferroni corrections. (D–F) Change in the response characteristics to a cooling ramp, of cold nerve terminals in control and tear-deficient corneas at different time points after surgery (control, n = 45; 1 week, n = 93; 2 weeks, n = 18; and 4 weeks, n = 57). (D) Cooling threshold (temperature decrease in degree Celsius that evokes a 25% increase in the firing frequency). (E) Ongoing NTI activity (mean discharge rate in imp/s) at 34°C. (F) Peak frequency (maximal response to cold in imp/s obtained during a cooling ramp). *$P < 0.05$, 1-way ANOVA with the Dunnett test. (G) Histogram showing the interval distribution of NTIs of cold nerve terminals from control and 4-week tear-deficient eyes (n = 30 in each group) during the maximal response to cold. The corresponding normal-fit curves are projected on histograms (dashed lines). Shorter interspike intervals were observed in tear-deficient nerve terminals. (H) Sample recording of a single cold sensitive nerve terminal in a tear-deficient cornea (4 weeks after surgery) during stepwise cooling. Upper channel: Instantaneous frequency (Hz); middle channel: firing rate (imp/s); lowest channel: temperature values (°C) of the perfusion solution along the record. (I) Mean NTI firing frequency (imp/s) of cold nerve terminals of control (n = 10) and tear-deficient corneas (n = 10) during stepwise cooling. In control corneas, the firing rate during the dynamic component of the NTI response (black squares) was significantly higher than during the static component of the NTI response (black circles, $P < 0.05$), whereas in tear-deficient corneas, these differences were not significant ($P = 0.125$). All the data are mean ± SEM.

We also analyzed the changes in Na^+ and K^+ currents observed in retrogradely labeled corneal TG neurons unresponsive to menthol, but activated by capsaicin and in most cases also by AITC, which were classified as corneal polymodal nociceptor neurons. Four weeks after lachrymal gland removal, TTX-r I_{Na} currents in polymodal nociceptor neurons innervating tear-

Table 3

Characteristics of spontaneous and cold-evoked nerve terminal impulse activity in control corneas and at different times after surgical removal of the lachrymal gland.

	Control (n = 45)	Time after lachrymal gland removal		
		1 wk (n = 93)	2 wk (n = 18)	4 wk (n = 57)
Ongoing activity (imp/s)	10.27 ± 0.78	10.50 ± 0.59	11.32 ± 1.35	13.22 ± 1.00*
Cooling threshold (°C)	29.87 ± 0.35	32.37 ± 0.13*	32.67 ± 0.33*	32.42 ± 0.14*
Peak frequency (imp/s)	25.29 ± 1.79	28.51 ± 1.37	29.47 ± 2.03	31.12 ± 1.80*
Temperature at peak frequency (°C)	27.46 ± 0.53	28.28 ± 0.33	30.33 ± 0.53	28.68 ± 0.28

Data are mean ± SEM; n = number of nerve terminals.
* $P < 0.05$, 1-way analysis of variance with the Dunnett test for differences from the control.

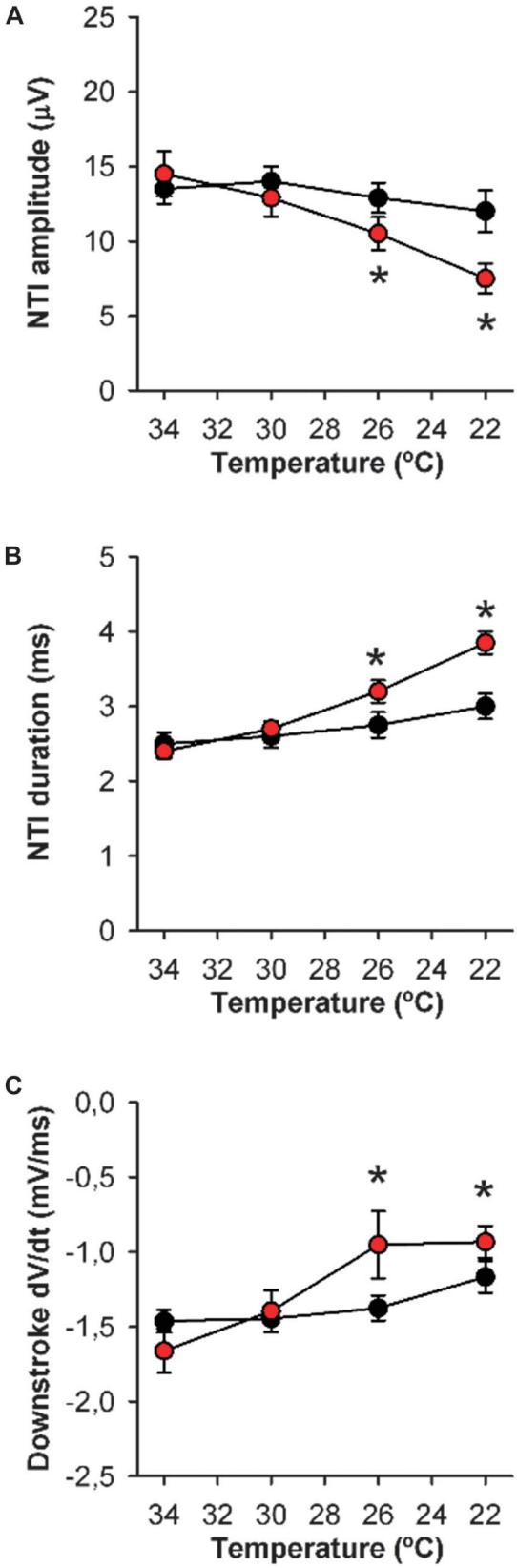

Figure 5. Changes in nerve terminal impulse (NTI) shape in cold nerve terminals of control and tear-deficient corneas. Parameters of 15 to 20 successive NTIs were measured in the same population of cold nerve terminals at 4 static temperatures in control (n = 10, black symbols) and in tear-deficient animals (n = 10, red symbols). (A) Mean amplitude. (B) Mean impulse duration. (C) Mean dV/dt measured during the downstroke phase of the nerve impulses. Data are mean ± SEM; *$P < 0.05$, *t* test, difference from values at 34°C.

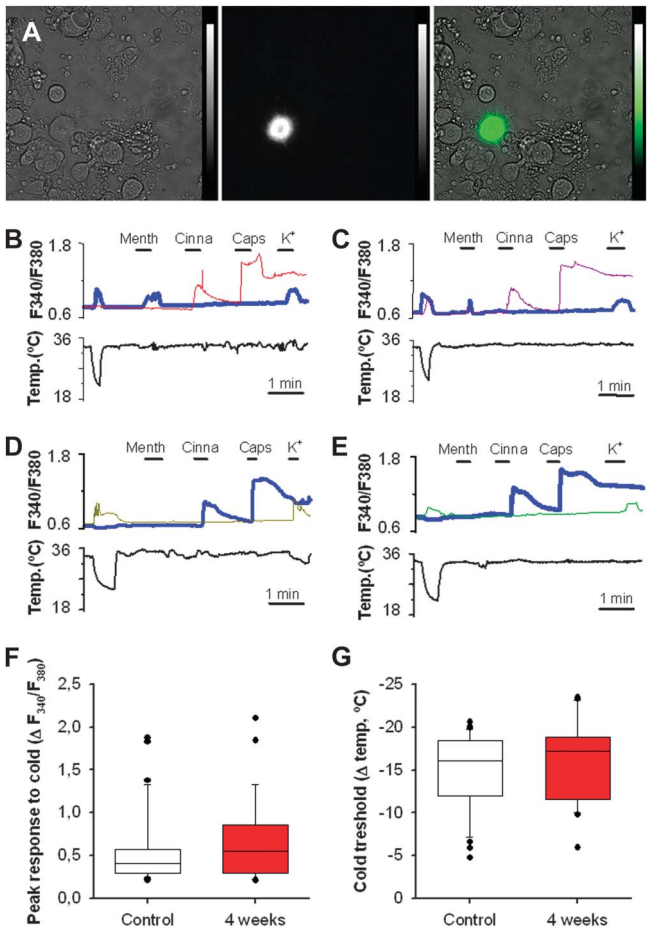

Figure 6. Intracellular calcium responses of trigeminal sensory neurons innervating the cornea of control and 4-week tear-deficient guinea pigs. (A) Trigeminal ganglion (TG) neurons innervating the cornea were retrogradely labeled with FM 1-43 applied on the corneal surface 6 days earlier and identified with fluorescence microscopy. Only one or 2 corneal neurons were found per culture plate. Photographs show (from left to right) bright field, FM 1-43 fluorescence when excited with 470-nm light and merged images. (B–E) Ratiometric fluorescence changes (expressed as the ratio of fluorescence of Fura-2 when excited at 340 and 380 nm, F_{340}/F_{380}) recorded simultaneously in the same culture plate from several fresh cultured TG sensory neurons from control (B and D) and tear-deficient (C and E) animals, in response to a cooling ramp and to the addition to the bath solution of 100 μM menthol, 100 μM cinnamaldehyde, 1 μM capsaicin, and 30 mM K^+; the bath temperature was simultaneously recorded (lower channels). The blue lines correspond to recordings from TG neurons innervating the cornea. Neurons responding to cooling and menthol were classified as cold thermosensitive neurons (B and C); neurons not responding to cooling stimulus but responding to capsaicin and cinnamaldehyde were classified as putative polymodal nociceptive neurons (D and E). (F) Box plots showing $[Ca^{2+}]_i$ peak response to cooling ramps (peak value of the F_{340}/F_{380} ratio during the ramp) in cold sensitive corneal neurons of control (n = 36; median = 0.40, range = 0.21-1.87) and tear-deficient animals (29; median = 0.55, range = 0.21-2.10). Horizontal line, median; bar, 25th and 75th interquartile range; whiskers, 10th and 90th percentiles. (G) Box plots showing $[Ca^{2+}]_i$ threshold response to cooling ramps (temperature decrease required to evoke the $[Ca^{2+}]_i$ response) in the same population of corneal neurons of control (n = 36; median = −16.06, range = −4.79 to −20.59) and tear-deficient animals (n = 29; median = −17.23, range = −5.94 to −23.46).

deficient eyes were not significantly different ($P = 0.501$; **Fig 11A**, **Table 4**) from those of intact animals. In contrast, a significant increase in TTX-s Na^+ currents ($P < 0.001$; 2-way ANOVA) was observed in such polymodal neurons, where significantly larger currents were activated at −30 and −20 mV (n = 6) when compared with those found in intact eyes (n = 8; **Fig. 11B**).

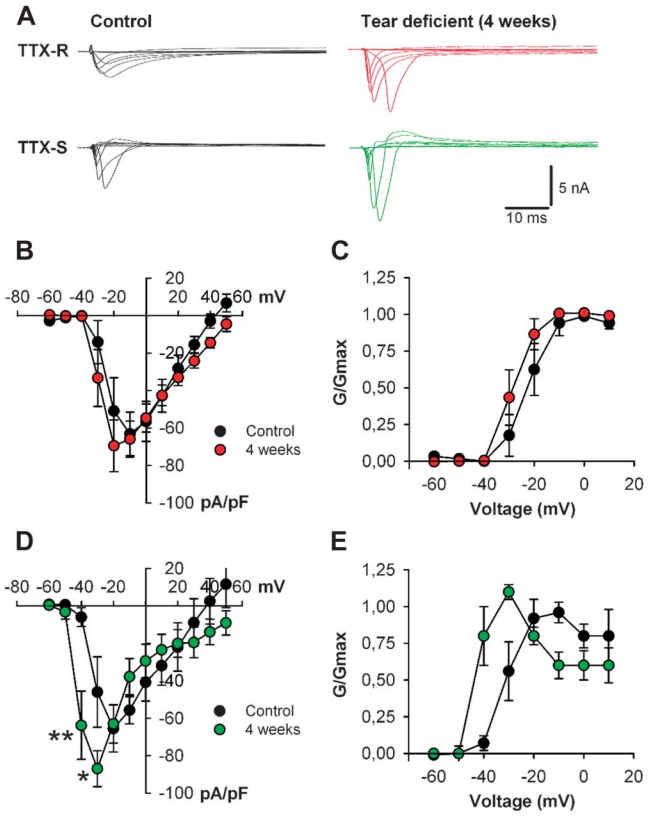

Figure 7. Voltage-gated Na^+ currents in trigeminal corneal cold sensory neurons of control and tear-deficient guinea pigs at 4 weeks after lachrymal gland removal. Corneal neurons were retrogradely labeled with FM 1-43 applied on the cornea 6 days earlier. (A) For each neuron, membrane potential was held at −80 mV; whole-cell sodium currents were evoked after a 500-millisecond prepulse to either −120 or −40 mV with a 100-millisecond step to potentials between −60 and +50 mV in 10 mV increments; current evoked from −40 mV was considered to be TTX-r current, whereas the difference between the current evoked from −120 and −40 mV was considered to be TTX-s; for clarity, only traces from −60 to +20 mV are shown. (B and C) Mean voltage–current relationships and mean relative peak conductance normalized to the maximal conductance (G/G_{max}) and plotted against voltage of TTX-r sodium currents. (D and E) Mean voltage–current relationships and mean relative peak conductance normalized to the maximal conductance (G/G_{max}) and plotted against voltage of TTX-s sodium currents. Data are mean ± SEM; $^{**}P < 0.01$; $^{*}P < 0.05$, *t* test.

Despite a slight leftward shift in the conductance–voltage relationship for TTX-s I_{Na} in neurons of tear-deficient eyes, differences did not reach statistical significance; the same was true for the slope factor (**Table 4**). Likewise, rapidly inactivating, slowly inactivating, and noninactivating K^+ currents were similar in operated (n = 15) and control animals (n = 12; data not shown).

Finally, we identified a population of retrogradely labeled corneal TG neurons that did not respond to any of the compounds tested (menthol, AITC, or capsaicin) but where depolarized by extracellular K^+ application. By exclusion, we considered these to be corneal mechanonociceptor neurons. The characteristics of Na^+ and K^+ currents in this subgroup of neurons from control and from tear-deficient animals were not statistically different (data not shown).

Table 4

Activation properties of voltage-gated Na^+ currents in corneal cold and polymodal sensory neurons from control and 4-week tear deficient animals.

	Cold		Polymodal	
	Control (n = 7)	4 wk (n = 7)	Control (n = 8)	4 wk (n = 6)
TTX-r				
$V_{0.5}$ (mV)	−21.9 ± 3.0	−29.0 ± 2.4*	−22.3 ± 3.5	−23.7 ± 1.6
Slope factor	1.9 ± 0.8	1.3 ± 0.5	1.5 ± 0.7	1.5 ± 0.7
TTX-s				
$V_{0.5}$ (mV)	−29.7 ± 2.8	−42.8 ± 1.9†	−35.8 ± 2.7	−31.6 ± 6.7
Slope factor	2.3 ± 1.2	1.3 ± 0.8	0.5 ± 0.1	0.7 ± 0.2

Data are mean ± SEM; n = number of recorded neurons.
* $P < 0.05$, *t* test.
† $P < 0.01$, *t* test.

3.4. Relationship between activation of corneal cold thermoreceptors and discomfort sensations in healthy subjects and patients with DED

Next, we tried to determine whether the unpleasant sensations experienced by humans when the eye surface is insufficiently humidified might be associated with changes in impulse activity of ocular cold thermoreceptors. We thus attempted to increase the impulse activity of cold receptor fibers in the ocular surface of healthy human volunteers and in patients with DED, using relatively specific stimuli for TRPM8 channels, such as menthol, cold saline, and air blown onto the eye, assessing in parallel the sensations experienced.

In the first place, we confirmed that, as expected, menthol (50-200 μM) effectively increased the ongoing and cold-evoked activity of corneal cold terminals, and augmented blinking frequency and tearing rate in vigilant intact and operated guinea pigs (**Fig. 12**). As shown in **Figure 12A**, the value of mean NTI peak frequency evoked by a cooling ramp in intact corneas (filled black column) increased significantly after application of 100 μM menthol (hatched black column). In tear-deficient corneas, the peak NTI response to a cold pulse ramp was significantly higher than in control animals (filled red column), whereas in the presence of 100 μM menthol, peak frequency values evoked by cooling pulses were significantly lower (hatched red bar). As shown in **Figure 12B**, black columns, basal spontaneous activity of cold nerve terminals (filled column) increased significantly with 100 μM menthol (hatched column) recovering after a 5-minute washing period (grid column). A similar effect but with an initially higher value of background activity was observed in tear-deficient corneas (**Fig. 12B**, red columns). Application of a higher menthol concentration (200 μM) evoked an initial increase in frequency followed by partial inactivation in both intact and tear-deficient corneal nerve terminals, as shown in **Figure 12C**. Also, increases in blinking frequency induced by 200 μM menthol were less pronounced in tear-deficient than in control guinea pigs (**Fig. 12D**). We also ascertained that at concentrations up to 200 μM (50-200 μM, n = 26), menthol did not evoke acute firing or the appearance of ongoing activity in polymodal nociceptor fibers of intact or tear-deficient guinea pig corneas (data not shown). Finally, we found that topical menthol (100 and 200 μM) and cold saline (2°C), did not evoke scratching or wiping movements in guinea pigs that are provoked by topical administration of the TRPV1 agonist capsaicin at 100 μM (data not shown).

Previous, preliminary experiments applying a 100 μM menthol solution on both eyes of healthy human subjects[11] had shown that this compound evoked a sensation of irritation and cooling. Nonetheless, the vehicle (containing 0.001% ethanol to dissolve the menthol) already produces mild irritation symptoms. Therefore, in the present experiments, menthol stimulation of cold sensory fibers of the human ocular surface was performed

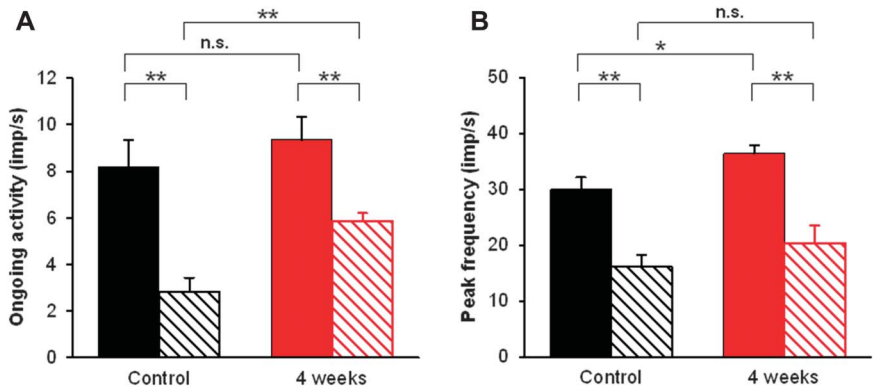

Figure 8. Effect of 100 nM hainantoxin-IV on the spontaneous and cold-evoked activity of corneal cold nerve terminals in control and tear-deficient corneas. (A) Effect of hainantoxin on the ongoing nerve terminal impulse activity of cold nerve terminals at basal temperature in control and tear-deficient corneas. (B) Effect of hainantoxin on the peak frequency of the discharge evoked by a cooling ramp in cold nerve terminals of control and tear-deficient corneas. Data are mean ± SEM, n = 6 in control and n = 4 in tear-deficient corneas; $^{*}P < 0.05$, $^{**}P < 0.001$, paired or unpaired *t* test, as needed.

indirectly through applying onto the cheekbone an ointment that released menthol vapors. The final menthol concentrations attained in the tear fluid, of the conjunctival sac, 4 minutes after applying ointments containing 1 mM and 10 mM menthol were 5 μM and 39.5 μM, respectively (see Methods). The effects of the menthol ointment were studied in healthy volunteers (age:

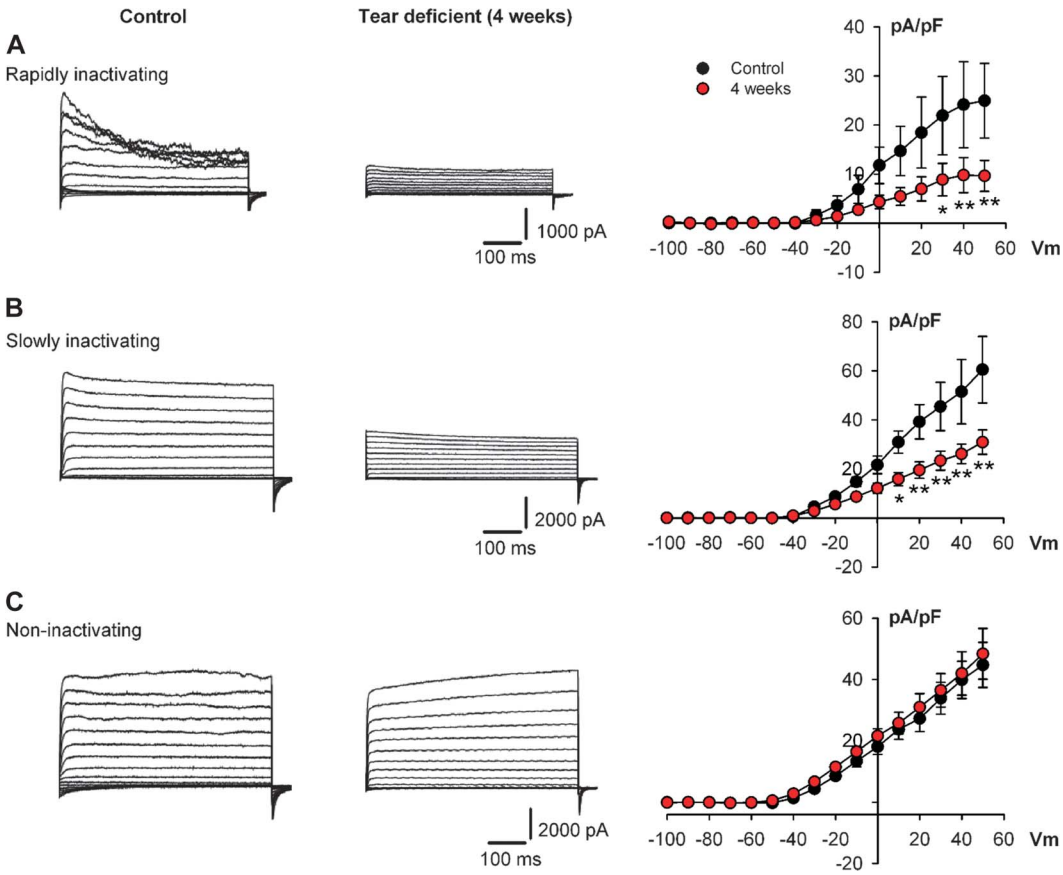

Figure 9. Voltage-gated K^+ currents (rapidly inactivating, slowly inactivating, and noninactivating currents) in control and tear-deficient trigeminal cold-sensitive neurons innervating the cornea. (A) Rapidly inactivating $K_{A,fast}$ currents obtained by subtraction of protocol 2 from protocol 1. Protocol 1: depolarizing voltage steps from −100 to +50 mV (500 milliseconds) made from −100 mV. Protocol 2: similar to protocol 1 but including a short depolarizing prepulse at −10 mV, 60 milliseconds to inactivate the rapidly inactivating component (see Methods). (B) Slowly inactivating $K_{A,slow}$ currents obtained by subtraction of currents elicited by protocol 3 from those obtained by protocol 2. In protocol 3, the same voltage steps were recorded but after a 7-second conditioning step to −10 mV to inactivate both the rapidly and slowly inactivating currents, leaving only the noninactivating and leak components. (C) Noninactivating currents obtained with protocol 3 in which the leak component was removed with a p/8 leak subtraction protocol. On the right side of the figure, the mean voltage–current relationships for the 3 types of K^+ currents (n = 5 for each group) are shown. Rapidly and slowly inactivating V–I curves showed statistically significant differences between control and tear-deficient neurons (repeated-measures analysis of variance, $P < 0.001$; post hoc comparison using a *t* test with Bonferroni corrections; $^{**}P < 0.001$, $^{*}P < 0.05$). Noninactivating currents did not show significant differences between groups.

Table 5

Activation and inactivation properties of voltage-gated K^+ currents in corneal cold sensory neurons from control and 4-week tear deficient animals.

	Control (n = 5)	4 wk (n = 5)
Activation		
Rapidly inactivating		
$V_{0.5}$ (mV)	−12.5 ± 2.0	−14.5 ± 7.6
Slope factor	7.9 ± 1.7	15.9 ± 6.0
Slowly inactivating		
$V_{0.5}$ (mV)	−8.6 ± 2.4	−10.6 ± 2.1
Slope factor	15.1 ± 2.2	17.2 ± 2.0
Noninactivating		
$V_{0.5}$ (mV)	−12.7 ± 1.9	−20.1 ± 3.2
Slope factor	16.8 ± 1.5	20.2 ± 2.5
Inactivation		
Rapidly inactivating		
$V_{0.5}$ (mV)	−45.9 ± 2.5	−64.2 ± 7.7*
Slope factor	−12.3 ± 2.2	−20.5 ± 9.0
Slowly inactivating		
$V_{0.5}$ (mV)	−36.3 ± 2.9	−35.9 ± 1.1
Slope factor	11.9 ± 3.2	6.8 ± 1.0

Data are mean ± SEM; n = number of recorded neurons.
* $P < 0.05$, *t* test.

33.3 ± 2.3, n = 18) and in patients with moderate DED (age: 43.6 ± 3.8, n = 9). The blink rate was determined 3 minutes after menthol application, whereas tear volume was measured 7 minutes later. Then, an assessment of the psychophysical parameters of the experienced sensations was performed (see Methods). The low-concentration (1 mM) menthol ointment evoked weak conscious sensations of cold and no significant unpleasantness or changes in the tearing rate in healthy volunteers, although their blink rate rose significantly (**Fig. 13**). By contrast, the high-concentration (10 mM) menthol ointment significantly increased the blink rate and the perception of discomfort and coolness measured with a VAS scale, reflecting the unpleasant nature of the sensation. No significant changes in the tearing rate were observed with any of these concentrations. A similar yet less pronounced response was obtained after exposing the eyes of healthy subjects and patients with DED to a room temperature air current (**Fig. 14**). Of note, in the group of patients with DED, the basal blink rate at rest was significantly higher than in healthy subjects ($P = 0.002$, *t* test) and was augmented by menthol. The most striking observation of menthol ointment application in patients with DED at both concentrations was that unpleasantness, which under basal conditions was rated to be higher than in healthy individuals, decreased. The sensation evoked by menthol in healthy subjects and patients with DED also included a component of coolness (**Figs. 13A and B**). Finally, the higher background discomfort in patients with DED was not further increased by exposure to an air current (**Fig. 14**).

4. Discussion

Together, our study proves that sustained increases of ocular cold thermoreceptor impulse activity mediated by enhanced Na^+ currents combined with diminished K^+ currents is the most prominent alteration of peripheral sensory input during prolonged experimental reduction of eye surface wetness. Changes in the responsiveness and membrane currents of polymodal nociceptor neurons, the presumed source of pain sensations in all body tissues,[57] seems to be comparatively less pronounced. We also found that selective stimulation of corneal cold sensory fibers in healthy humans evokes distinct sensations of eye discomfort, which reinforces the suggestion that the population of cold thermoreceptors could play an important role in signaling potentially injurious desiccation of the ocular surface.[8]

In mammals, low-threshold cold thermoreceptors have been hitherto considered specific sensors of environmental temperature reductions.[34] However, our recent evidence has shown that moderate elevations of tear osmolality, as those occurring during eye surface evaporation, act directly on TRPM8 channels and increase corneal cold thermoreceptor activity.[59,63] Hence, we now propose that in addition to the canonical role of signalling body surface temperature decreases attributed to cold thermoreceptors, this seem to provide also information about the wetness level of the eye surface and possibly of other exposed body mucosae, reminiscent of thermosensitive "hygroreceptors" of the sensory antennae of insects,[71] eventually evoking conscious sensations, and compensatory changes in tearing and blink rate.

We noticed that after a long-lasting experimental tearing reduction, the axonal arborizations in the uppermost layers of the guinea pig corneal epithelium, which are subjected to continuous regeneration and remodeling,[33] appeared morphologically altered. Anatomical abnormalities have been also reported in the subbasal corneal nerves of patients with DED,[12] possibly reflecting nerve injury secondary to the chronic physical trauma exerted on ocular surface epithelial cells and the local inflammatory reaction evoked by prolonged surface dryness.[22,24] Altered sodium and potassium currents are characteristic of peripheral sensory nerve damage.[21,23] Our data suggest that injury-induced disturbances in these currents rather than in cold-transducing TRPM8 current are behind the enhanced responsiveness to low temperatures of cold sensory nerve terminals gradually developing in tear-deficient corneas.[42,43] Such excitability disturbances were largely restricted to cold neurons and have similitudes with those produced for instance by the neurotoxic chemotherapy agent oxaliplatin, which causes peripheral damage of cutaneous nerve terminals and cold allodynia; oxaliplatin impairs the expression of channels that modulate cold thermoreceptor neuronal activity, enhancing TTX-s, resurgent, and persistent Na^+ currents evoked by cooling, whereas the expression of TRPM8 was unaffected.[19,66] In corneal cold thermoreceptor neurons, ocular dryness increased TTX-s Na^+ currents while decreasing the rapidly inactivating and slowly inactivating K^+ currents. Altogether, these effects are likely to move the firing threshold towards higher temperatures, enhancing thermoreceptor impulse activity. In contrast, nociceptors appear less altered and only TTX-s Na^+ currents in corneal polymodal nociceptor neurons appeared augmented, whereas TTX-r and K^+ currents were not significantly changed. This is in agreement with the weak sensitization found in mechanonociceptor and polymodal nociceptor fibers of tear-deficient guinea pig eyes. It is doubtful that inflammatory mediators responsible for such sensitization also contribute to the hyperexcitability displayed by cold thermoreceptors; inflammatory substances actually reduce basal and stimulus-evoked firing of corneal cold thermoreceptors through direct inhibition of TRPM8 channels.[4,80]

Menthol, which increased the ongoing and cold-evoked activity of corneal cold thermoreceptors but had no effect on corneal polymodal nociceptors of control guinea pig eyes, also evoked conscious eye discomfort sensations and augmented blinking in healthy human subjects. This further supports the hypothesis that a heightened sensory input from eye surface cold thermoreceptors to the brain importantly contributes to the sustained unpleasant sensations and blinking and tearing rate

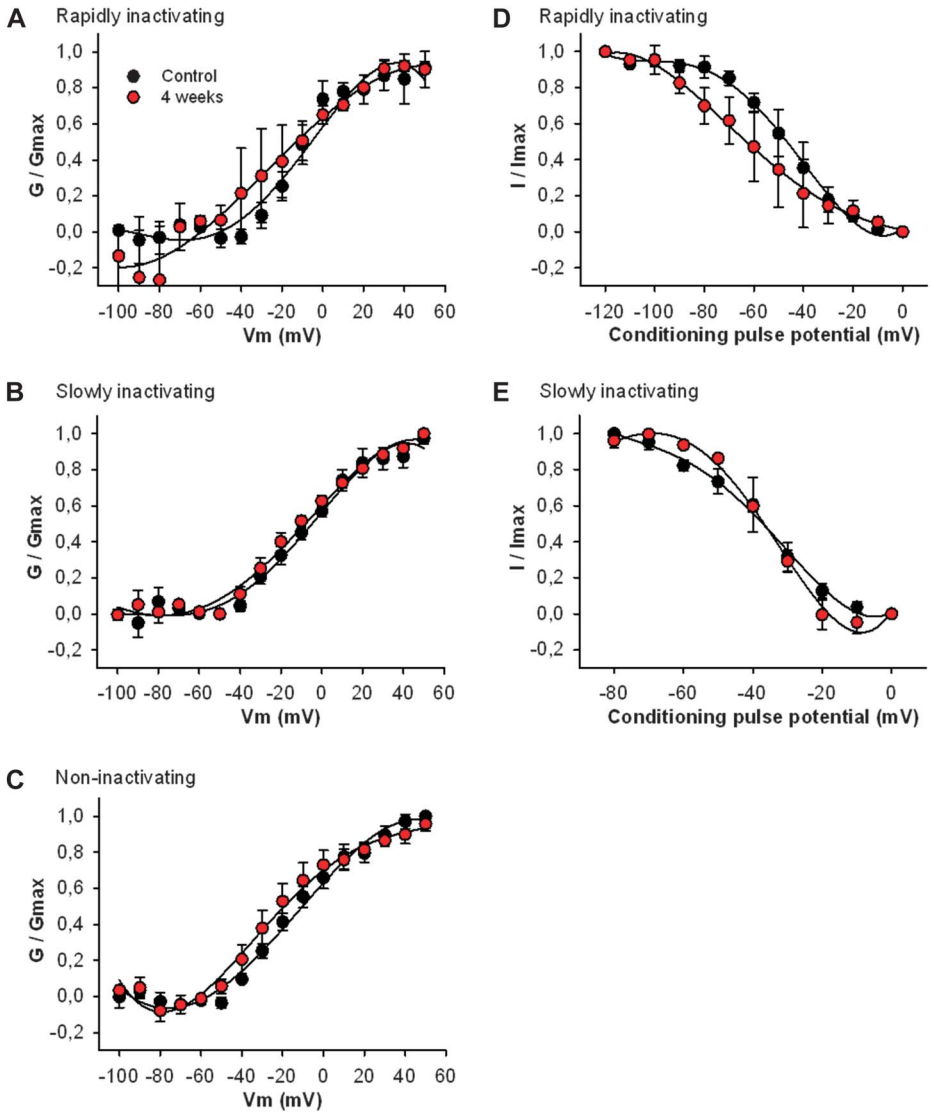

Figure 10. Activation and inactivation curves of voltage-gated K^+ currents in corneal cold sensory neurons from control and 4-week tear-deficient guinea pigs. Activation curves were generated by voltage pulses in 10-mV steps from −100 to +50 mV. Activation voltage dependency was studied by plotting normalized conductance (G/G_{max}) against test pulse voltage, and the data were fitted using a Boltzmann function. (A) Activation curves for rapidly inactivating K^+ current in cold sensory neurons from control and tear-deficient animals (n = 5 neurons in each group). $V_{0.5}$: control −12.5 ± 2.0 mV; tear-deficient −14.5 ± 7.6 mV. Slope factor: control 7.9 ± 1.7; tear-deficient 15.9 ± 6.0. No significant differences were observed. (B) Activation curves for slowly inactivating K^+ current (n = 5 neurons each) $V_{0.5}$: control −8.6 ± 2.4 mV; tear-deficient −10.6 ± 2.1 mV. Slope factor: control 15.1 ± 2.2; tear-deficient 17.2 ± 2.0. (C) Activation curves for noninactivating K^+ current (n = 5 neurons in each group), $V_{0.5}$: control −12.7 ± 1.5 mV; tear-deficient −20.1 ± 2.5 mV. Slope factor: control 16.8 ± 1.5; tear-deficient 20.2 ± 2.5. (D) Inactivation curves for rapidly inactivating K^+ current. Inactivation curves were constructed using a 2-pulse protocol, a 1-second prepulse varying between −120 and 0 mV, followed by a 400-millisecond test pulse of +50 mV. The peak of the transient component was measured. Tear-deficient neurons showed a significant leftward shift in the inactivation curve of $K_{A,fast}$ ($P < 0.05$, 1-way repeated-measures analysis of variance). $V_{0.5}$: control −45.9 ± 2.5 mV, tear-deficient −64.2 ± 7.7 mV. Slope factor: control −12.3 ± 2.2, tear-deficient −20.5 ± 9.0. (E) Inactivation curves for slowly inactivating $K_{A,slow}$ were constructed using a 2-pulse protocol: an 8-second prepulse varying between −80 and 0 mV followed by a 1-second test pulse of +50 mV. No significant effects were observed between groups.

adjustments occurring during eye dryness.[59,63] Menthol effects on cold thermoreceptors are mediated through the opening of TRPM8 channels.[45,55,61,62] However, this drug is very promiscuous and acts also as an inhibitor of TRPA1, a transduction channel expressed by polymodal nociceptor neurons exhibiting sensitivity to intense cold.[51,77,79] Thus, the possibility that menthol affects other channels in polymodal fibers cannot be completely excluded. However, human TRPA1 is insensitive to the inhibitory effects of menthol.[77] Moreover, we confirmed that at the concentrations reached in our human experiments, menthol did not act in corneal polymodal nociceptor fibers of the guinea pigs. This reinforces the conclusion that unpleasant sensations evoked by menthol applied to the healthy human ocular surface are mediated predominantly, and perhaps exclusively through a concentration-dependent activation of TRPM8-expressing eye surface cold thermoreceptor fibers. In intact guinea pig cornea, menthol at low concentrations (<200 μM) strongly activates cold thermoreceptor fibers, whereas higher concentrations depress such activity after an initial, transient excitatory period.[43,60] A previous study in healthy human eyes reported that 1 mM menthol caused an immediate and transient feeling of cooling and mild irritation, followed by long-lasting selective suppression of corneal sensitivity to cold.[3]

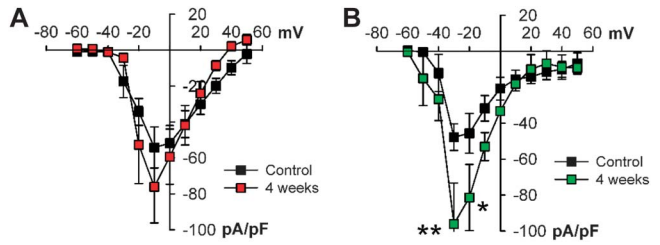

Figure 11. Voltage-gated Na^+ currents in trigeminal polymodal sensory neurons of control and tear-deficient guinea pigs 4 weeks after lachrymal gland removal. Corneal neurons were retrogradely labeled with FM 1-43 applied on the cornea 6 days earlier. Mean voltage–current relationships for TTX-r (A) and TTX-s (B) sodium currents. Data are mean ± SEM; $^{**}P < 0.01$; $^{*}P < 0.05$, *t* test.

Trigeminal neurons with the phenotype of specific cold thermoreceptors exhibit an ample range of thermal and menthol thresholds.[52,70] Such threshold differences are due to a variable expression of TRPM8 and of cold-sensitive Kv1 channels whose IK_D current opposes cold-induced depolarization.[32,41,52,75] In our experiments in humans using an ointment containing 1 mM menthol, a low concentration of the drug was detected in the tear film, which suggests that under these conditions, only the fraction of lowest threshold cold thermoreceptors was activated. Of note, this caused a significant increase in the basal blink rate, which depends on TRPM8-expressing cold thermoreceptor fibers[63] but did not produce an augmented tearing and evoked only weak conscious sensations, with a predominant thermal component. Notably, a higher menthol concentration in the ointment, which expectedly recruits a larger number of cold thermoreceptor fibers, evoked a sensation containing a distinct discomfort component. We cannot exclude the possibility that such unpleasantness appears when the subpopulation of polymodal nociceptors expressing TRPA1 and connected centrally with pain-labelled lines is recruited,[16,47,50,79] although most canonical polymodal nociceptor fibers of the cornea seem to be insensitive to intense cold.[10] However, in the skin, a fraction of sensory fibers exhibiting sensitivity to menthol and cold, combined with responsiveness to capsaicin and/or AITC have been identified.[40] Likewise, a small number of TRPM8-expressing thermoreceptor fibers, with no spontaneous activity at background corneal temperatures, responding to menthol and intense cooling have been recently described in the mouse cornea.[38] Whether these belong to the group of highest threshold cold thermoreceptors[70] or to the subset of TRPM8-expressing polymodal nociceptors found in the skin[58] cannot be answered yet.

Notably, in patients with moderate DED, menthol attenuated the subjective indicators of unpleasantness that were already present under basal conditions, in contrast to healthy individuals. Likewise, topical application of menthol to the healthy skin of patients with neuropathy evoked cold allodynia, whereas in a mirror neuropathic skin area, menthol attenuated the preexisting cold allodynia.[76] Recent evidence in the rat has shown that menthol concentrations over 0.5 mM are required in intact eyes to evoke long-lasting inhibition of corneal cold thermoreceptor activity, whereas in tear-deficient animals, inhibition was already obtained with values under 100 μM.[43] Hence, alleviation of basal unpleasant dryness sensations experienced by patients with DED when treated with menthol concentrations causing discomfort in healthy eyes can be attributed, at least in part, to an attenuation of the augmented cold thermoreceptor ongoing firing, expectedly present in human chronic tear-deficient corneas. This inhibition could be the consequence of a use-dependent depression of

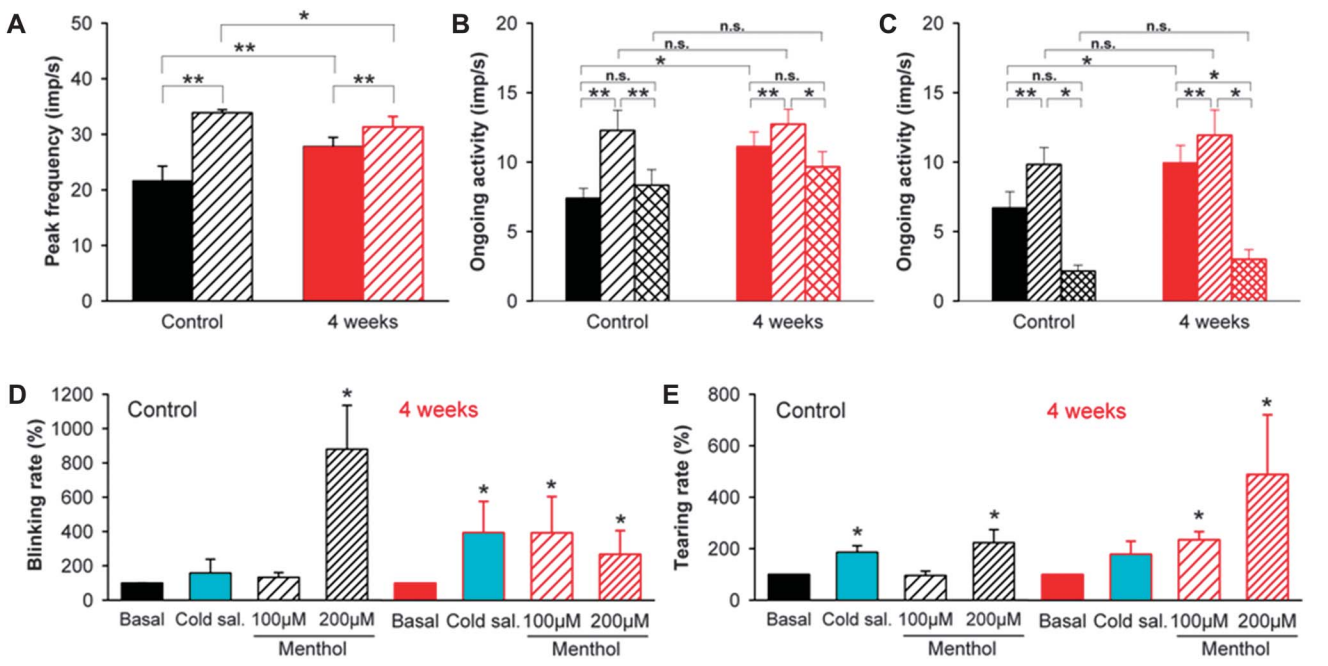

Figure 12. Effects of menthol on the spontaneous and cold-evoked nerve terminal impulse (NTI) firing frequency of cold nerve terminals, blinking frequency, and tearing rate, in control (red columns) and tear-deficient animals (red columns) 4 weeks after surgical removal of the lachrymal gland. (A) Effect of menthol on the NTI peak frequency value of the response evoked by cooling ramps to 20°C, in cold nerve terminals of control and tear-deficient corneas. (B and C) Effect of 100 μM (B) and 200 μM (C) menthol on the ongoing NTI activity in control (n = 17, black) and tear-deficient (n = 15, red) cold nerve terminals at the basal temperature of 34°C. The bars represent ongoing activity before (full bars), during (hatched bars), and 5 minutes after perfusion with menthol (double hatched bars). $^{**}P < 0.001$, $^{*}P < 0.05$, paired or unpaired *t* test, as needed. (D and E) Effect on blinking frequency and tearing rate of topical application of ice-cold saline and 100 μM and 200 μM menthol solutions in control and tear-deficient animals. Data are mean ± SEM of the change in the measured parameter, expressed as % of the basal value; n = 6 in each group; $^{*}P < 0.05$, paired *t* test.

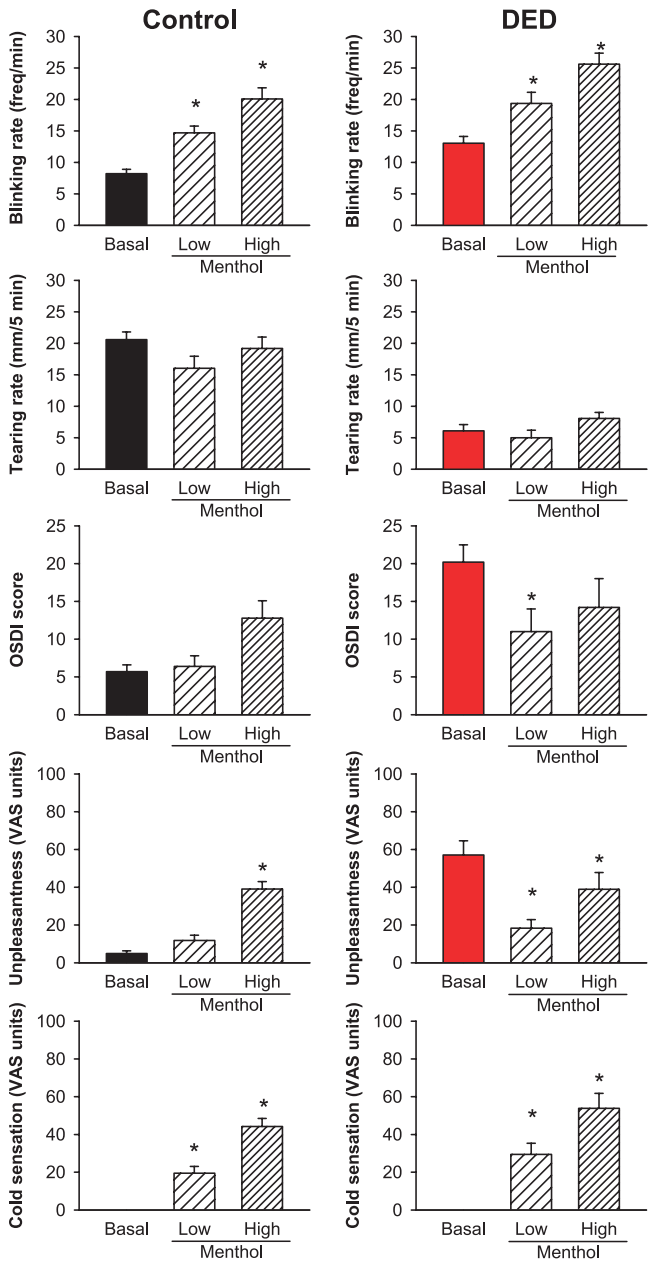

Figure 13. Effects of menthol on blinking frequency, tearing rate, and ocular sensation parameters in control and patients with dry eye disease (DED). Menthol was applied as an ointment onto the cheekbone skin at 1 and 10 mM concentrations (leading respectively to 5 and 39.5 μM menthol concentrations in tears). Data from control subjects (n = 18) and patients with DED (n = 9) are shown. From top to bottom: Mean blinking frequency measured off-line from webcam recordings performed during 3 minutes; tearing rate measured with commercial Schirmer strips without anesthesia during 5 minutes; Ocular Surface Disease Index (OSDI) score measured with a questionnaire approved for Spanish-speaking people; unpleasantness sensation measured with a 0-to-100 visual analog scale (VAS); cold sensation intensity measured with a 0-to-100 VAS. $P < 0.001$, repeated-measures Analysis of variance with post hoc analysis using the Bonferroni t test (*$P < 0.001$).

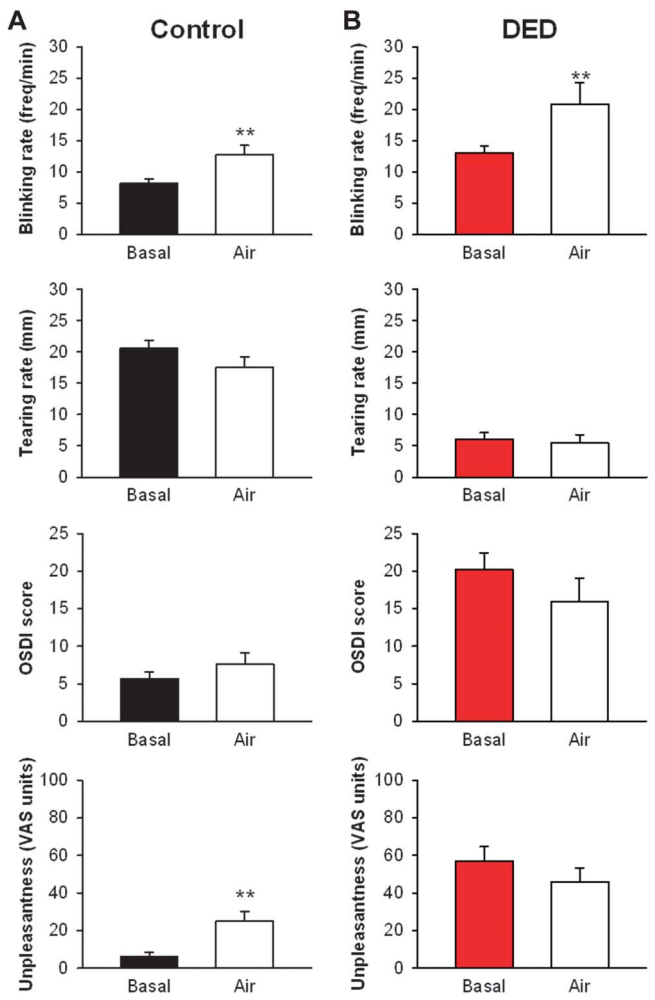

Figure 14. Effect of ocular surface dryness induced by an air stream directed to the face on blinking frequency, tearing rate, and ocular sensations in (A) control subjects and (B) patients with dry eye disease (DED). The following parameters were measured: mean blinking frequency measured off-line from video recordings of 3-minute duration; tearing rate, measured with Schirmer strips without anesthesia during 5 minutes; Ocular Surface Disease Index (OSDI) score determined with a questionnaire validated for Spanish-speaking people; unpleasantness sensation intensity scored with a 0-to-100 visual analog scale (VAS). Data are mean ± SEM, n = 18 control and n = 9 patients with DED; **$P < 0.001$, paired t test.

sodium channel activity in cold thermoreceptor fibers, reportedly caused by menthol.[26]

Altogether, the present data suggest that under comfortable environmental conditions, background activity in low-threshold cold thermoreceptors, the only afferent tonic input produced by corneal nerves, helps to maintain basal tearing[60] and spontaneous blinking,[63] but it is probably too weak to evoke conscious sensations of cooling or dryness. This background sensory input builds up critically with ocular surface temperatures decreases, as those occurring under exposure to extreme low temperatures, cold air, or evaporation in very dry environments. Augmented firing and recruitment of higher threshold cold thermoreceptors would evoke an unpleasant and qualitatively distinct sensation, consciously defined as unpleasant irritating dryness.[6] Conceivably, a similar response is already triggered by less drastic cooling when the tear film is too thin or abnormal, as occurs in patients with aqueous-deficient and evaporative DED. In such cases, ongoing cold thermoreceptor activity is expected to be high and further potentiated by the rise in tear fluid osmolality that accompanies enhanced evaporation[13,37,48,59] and is developed in experimental dry eye models reducing tear volume.[28] Damage to corneal nerve terminals due to long-term reduction of ocular surface wetness, as observed in guinea pig dry eye corneas, possibly confers neuropathic characteristics to the augmented activity of cold thermoreceptors, thereby perpetuating the initial

sensations of discomfort.[20,65] Recruitment of nociceptors by ocular surface injury and inflammation[7] possibly aggravates the unpleasant and distressing nature of the final sensation experienced by patients with DED.

In summary, cold thermoreceptors could be envisaged as the afferent branch of a specific alerting sensory circuit to maintain the equilibrium of ocular surface wetness, despite environmental oscillations in temperature and humidity. Such a mechanism would work in parallel with the conventional nocifensive system evoking pain and aimed to protect the eye from external injury, whose peripheral component corresponds to the canonical nociceptive afferents. Accordingly, dysfunction of the neural mechanisms regulating wetness would be, at least partly, behind the characteristic unpleasant dryness sensations reported by patients with DED, the most significant and disturbing symptom of this disease.

Conflict of interest statement

Commercial relationship: C. Belmonte and J. Gallar are authors of a patent (ES2377785, US9095609) that could be affected indirectly by this publication. The other authors have no conflicts of interest to declare.

This work was supported by the Spanish Ministerio de Economía y Competitividad, projects SAF2014-54518-C3-1-R and SAF2011-22500 (J.G.), and in part by SAF2014-54518-C3-2-R and BFU2008-04425 (C.B.), BFU2012-36845 and RETICS RD12/0034/0010 (N.C.), FIS PI11/01601, FIS PI14/00141, 2014SGR1165, and RD12/0034/0003 (X.G.), Fundación María Cristina Masaveu Peterson and PI FIS 110288 (J.M.-L. and C.B.), and by the Hungarian Scientific Research Fund—European FP7 Marie Curie Mobility grant Human-MB08A 80372 and OTKA NN106649 (I.K.).

Acknowledgements

The authors thank Manuel Bayonas and Ana Miralles for their skillful technical assistance, Enoch Luis and Javier Belmonte for their help with calcium imaging analysis and human experiments, respectively, and Héctor González for measuring menthol concentration in tears.

Author contribution: C. Luna and S. Quirce contributed equally to the work presented here and should therefore be regarded as equivalent authors. X. Gasull, C. Belmonte, and J. Gallar contributed equally to this work.

Article history:
Received 1 September 2015
Received in revised form 9 October 2015
Accepted 28 October 2015
Available online 15 December 2015

References

[1] Abdulla FA, Smith PA. Axotomy- and autotomy-induced changes in Ca2+ and K+ channel currents of rat dorsal root ganglion neurons. J Neurophysiol 2001;85:644–58.
[2] Abdulla FA, Smith PA. Changes in Na(+) channel currents of rat dorsal root ganglion neurons following axotomy and axotomy-induced autotomy. J Neurophysiol 2002;88:2518–29.
[3] Acosta MC, Belmonte C, Gallar J. Sensory experiences in humans and single unit activity in cats evoked by polymodal stimulation of the cornea. J Physiol 2001;534:511–25.
[4] Acosta MC, Luna C, Quirce S, Belmonte C, Gallar J. Changes in impulse activity of ocular surface sensory nerves during allergic keratoconjunctivitis. PAIN 2013;154:2353–62.
[5] Acosta MC, Luna C, Quirce S, Belmonte C, Gallar J. Corneal sensory nerve activity in an experimental model of UV keratitis. Invest Ophthalmol Vis Sci 2014;55:3403–12.
[6] Begley C, Simpson T, Liu H, Wu Z, Bradley A, Situ P. Quantitative analysis of tear film fluorescence and discomfort during tear film instability and thinning. Invest Ophthalmol Vis Sci 2013;54:2645–53.
[7] Belmonte C, Acosta MC, Merayo-Lloves J, Gallar J. What causes eye pain? Curr Ophthalmol Rep 2015;3:111–21.
[8] Belmonte C, Gallar J. Cold thermoreceptors, unexpected players in tear production and ocular dryness sensations. Invest Ophthalmol Vis Sci 2011;52:3888–92.
[9] Belmonte C, Gallar J, Pozo MA, Rebollo I. Excitation by irritant chemical substances of sensory afferent units in the cat's cornea. J Physiol 1991; 437:709–25.
[10] Belmonte C, Giraldez F. Responses of cat corneal sensory receptors to mechanical and thermal stimulation. J Physiol 1981;321:355–68.
[11] Belmonte J, Alfaro S, Berenguer TB, Costa JM, Cuquerella V, Acosta MC, Belmonte C, Gallar J. Effects of the TRPM8 agonist menthol on corneal sensitivity and tear secretion. Invest Ophthalmol Vis Sci 2010;51:E-Abstract 3405.
[12] Benítez-Del-Castillo JM, Acosta MC, Wassfi MA, Díaz-Valle D, Gegúndez JA, Fernandez C, García-Sánchez J. Relation between corneal innervation with confocal microscopy and corneal sensitivity with noncontact esthesiometry in patients with dry eye. Invest Ophthalmol Vis Sci 2007; 48:173–81.
[13] Benjamin WJ, Hill RM. Human tears: osmotic characteristics. Invest Ophthalmol Vis Sci 1983;24:1624–26.
[14] Brock JA, McLachlan EM, Belmonte C. Tetrodotoxin-resistant impulses in single nerve terminals signalling pain. J Physiol 1998;512:211–17.
[15] Brock JA, Pianova S, Belmonte C. Differences between nerve terminal impulses of polymodal nociceptors and cold sensory receptors of the guinea-pig cornea. J Physiol 2001;533:493–501.
[16] Campero M, Baumann TK, Bostock H, Ochoa JL. Human cutaneous C fibres activated by cooling, heating and menthol. J Physiol 2009;587: 5633–52.
[17] Dartt DA. Neural regulation of lachrymal gland secretory processes: relevance in dry eye diseases. Prog Retin Eye Res 2009;28:155–77.
[18] De la Peña E, Mälkiä A, Cabedo H, Belmonte C, Viana F. The contribution of TRPM8 channels to cold sensing in mammalian neurones. J Physiol 2005;567:415–26.
[19] Descoeur J, Pereira V, Pizzoccaro A, Francois A, Ling B, Maffre V, Couette B, Busserolles J, Courteix C, Noel J, Lazdunski M, Eschalier A, Authier N, Bourinet E. Oxaliplatin-induced cold hypersensitivity is due to remodelling of ion channel expression in nociceptors. EMBO Mol Med 2011;3:266–78.
[20] Devor M. Neuropathic pain: pathophysiological response of nerves to injury. In: McMahon SB, Koltzenburg M, Tracey I, Turk DC, editors. Wall and Melzack's textbook of pain. 6th ed. Philadelphia: Elsevier Saunders, 2013. p. 861–88.
[21] Dib-Hajj SD, Cummins TR, Black JA, Waxman SG. Sodium channels in normal and pathological pain. Annu Rev Neurosci 2010;33:325–47.
[22] Enríquez-de-Salamanca A, Castellanos E, Stern ME, Fernández I, Carreño E, García-Vázquez C, Herreras JM, Calonge M. Tear cytokine and chemokine analysis and clinical correlations in evaporative-type dry eye disease. Mol Vis 2010;16:862–73.
[23] Everill B, Kocsis JD. Reduction in potassium currents in identified cutaneous afferent dorsal root ganglion neurons after axotomy. J Neurophysiol 1999;82:700–8.
[24] Gallar J, Pozo MA, Tuckett RP, Belmonte C. Response of sensory units with unmyelinated fibres to mechanical, thermal and chemical stimulation of the cat's cornea. J Physiol 1993;468:609–22.
[25] García-Catalán MR, Jerez-Olivera E, Benítez-Del-Castillo-Sánchez JM. Dry eye and quality of life. Arch Soc Esp Oftalmol 2009;84:451–8.
[26] Gaudioso C, Hao J, Martin-Eauclaire MF, Gabriac M, Delmas P. Menthol pain relief through cumulative inactivation of voltage-gated sodium channels. PAIN 2012;153:473–84.
[27] Gilbard JP, Carter JB, Sang DN, Refojo MF, Hanninen LA, Kenyon KR. Morphologic effect of hyperosmolarity on rabbit corneal epithelium. Ophthalmology 1984;91:1205–12.
[28] Gilbard JP, Rossi SR, Gray KL, Hanninen LA, Kenyon KR. Tear film osmolarity and ocular surface disease in two rabbit models for keratoconjunctivitis sicca. Invest Ophthalmol Vis Sci 1988;29:374–8.
[29] Gold MS, Shuster MJ, Levine JD. Characterization of six voltage-gated K+ currents in adult rat sensory neurons. J Neurophysiol 1996;75: 2629–46.
[30] Gold MS, Weinreich D, Kim CS, Wang R, Treanor J, Porreca F, Lai J. Redistribution of Na(V)1.8 in uninjured axons enables neuropathic pain. J Neurosci 2003;23:158–66.

[31] Gold MS, Zang L, Wrigley DL, Traub RJ. Prostaglandin E2 modulates TTX-R INa in rat colonic sensory neurons. J Neurophysiol 2002;88: 1512–22.
[32] Green BG, Akirav C. Threshold and rate sensitivity of low-threshold thermal nociception. Eur J Neurosci 2010;31:1637–45.
[33] Harris LW, Purves D. Rapid remodeling of sensory endings in the corneas of living mice. J Neurosci 1989;9:2210–4.
[34] Hensel H, Andres KH, von Düring M. Structure and function of cold receptor. Pflugers Arch 1974;352:1–10.
[35] Hirata H, Fried N, Oshinsky ML. Quantitative characterization reveals three types of dry-sensitive corneal afferents: pattern of discharge, receptive field, and thermal and chemical sensitivity. J Neurophysiol 2012;108:2481–93.
[36] Hirata H, Meng ID. Cold-sensitive corneal afferents respond to a variety of ocular stimuli central to tear production: implications for dry eye disease. Invest Ophthalmol Vis Sci 2010;51:3969–76.
[37] Hirata H, Rosenblatt MI. Hyperosmolar tears enhance cooling sensitivity of the corneal nerves in rats: possible neural basis for cold-induced dry eye pain. Invest Ophthalmol Vis Sci 2014;55:5821–33.
[38] Íñigo-Portugués A, Alcalde I, Gonzalez-Gonzalez O, Gallar J, Merayo-Lloves J, Belmonte C. Effects of aging on neurochemical properties of mouse corneal cold sensory neurons, changes in morphology in their afferent projections and implications in basal tear secretion. Invest Ophthalmol Vis Sci 2015;56:E-Abstract 0290.
[39] Ivanusic JJ, Wood RJ, Brock JA. Sensory and sympathetic innervation of the mouse and guinea pig corneal epithelium. J Comp Neurol 2013;521: 877–93.
[40] Knowlton WM, Bifolck-Fisher A, Bautista DM, McKemy DD. TRPM8, but not TRPA1, is required for neural and behavioral responses to acute noxious cold temperatures and cold-mimetics in vivo. PAIN 2010;150: 340–50.
[41] Knowlton WM, Palkar R, Lippoldt EK, McCoy DD, Baluch F, Chen J, McKemy DD. A sensory-labeled line for cold: TRPM8-expressing sensory neurons define the cellular basis for cold, cold pain, and cooling-mediated analgesia. J Neurosci 2013;33:2837–48.
[42] Kovacs I, Quirce S, Luna C, Acosta MC, Belmonte C, Gallar J. Increased responsiveness of corneal cold receptors in an experimental model of dry eye. Invest Ophthalmol Vis Sci 2010;51:E-Abstract 3403.
[43] Kurose M, Meng ID. Dry eye modifies the thermal and menthol responses in rat corneal primary afferent cool cells. J Neurophysiol 2013;110: 495–504.
[44] Lam H, Bleiden L, de Paiva CS, Farley W, Stern ME, Pflugfelder SC. Tear cytokine profiles in dysfunctional tear syndrome. Am J Ophthalmol 2009; 147:198–205.
[45] Latorre R, Brauchi S, Madrid R, Orio P. A cool channel in cold transduction. Physiology (Bethesda) 2011;26:273–85.
[46] Lemp MA, Bron AJ, Baudouin C, Benítez Del Castillo JM, Geffen D, Tauber J, Foulks GN, Pepose JS, Sullivan BD. Tear osmolarity in the diagnosis and management of dry eye disease. Am J Ophthalmol 2011; 151:792–8.
[47] Lippoldt EK, Elmes RR, McCoy DD, Knowlton WM, McKemy DD. Artemin, a glial cell line-derived neurotrophic factor family member, induces TRPM8-dependent cold pain. J Neurosci 2013;33:12543–52.
[48] Liu H, Begley C, Chen M, Bradley A, Bonanno J, McNamara NA, Nelson JD, Simpson T. A link between tear instability and hyperosmolality in dry eye. Invest Ophthalmol Vis Sci 2009;50:3671–9.
[49] Luther JA, Birren SJ. Nerve growth factor decreases potassium currents and alters repetitive firing in rat sympathetic neurons. J Neurophysiol 2006;96:946–58.
[50] Ma Q. Labeled lines meet and talk: population coding of somatic sensations. J Clin Invest 2010;120:3774–8.
[51] Macpherson LJ, Hwang SW, Miyamoto T, Dubin AE, Patapoutian A, Story GM. More than cool: promiscuous relationships of menthol and other sensory compounds. Mol Cell Neurosci 2006;32:335–43.
[52] Madrid R, de la Peña E, Donovan-Rodriguez T, Belmonte C, Viana F. Variable threshold of cold-sensitive neurons is determined by a balance between TRPM8 and Kv1 potassium channels. J Neurosci 2009;29: 3120–31.
[53] Marfurt CF, Cox J, Deek S, Dvorscak L. Anatomy of the human corneal innervation. Exp Eye Res 2010;90:478–92.
[54] McFarlane S, Cooper E. Kinetics and voltage dependence of A-type currents on neonatal rat sensory neurons. J Neurophysiol 1991;66: 1380–91.
[55] McKemy DD, Neuhausser WM, Julius D. Identification of a cold receptor reveals a general role for TRP channels in thermosensation. Nature 2002; 416:52–8.
[56] Mengher LS, Pandher KS, Bron AJ. Non-invasive tear film break-up time: sensitivity and specificity. Acta Ophthalmol (Copenh) 1986;64:441–4.
[57] Olausson B. Recordings of polymodal single c-fiber nociceptive afferents following mechanical and argon-laser heat stimulation of human skin. Exp Brain Res 1998;122:44–54.
[58] Palkar R, Lippoldt EK, McKemy DD. The molecular and cellular basis of thermosensation in mammals. Curr Opin Neurobiol 2015;34:14–9.
[59] Parra A, Gonzalez-Gonzalez O, Gallar J, Belmonte C. Tear fluid hyperosmolality increases nerve impulse activity of cold thermoreceptor endings of the cornea. PAIN 2014;155:1481–91.
[60] Parra A, Madrid R, Echevarria D, del Olmo S, Morenilla-Palao C, Acosta MC, Gallar J, Dhaka A, Viana F, Belmonte C. Ocular surface wetness is regulated by TRPM8-dependent cold thermoreceptors of the cornea. Nat Med 2010;16:1396–9.
[61] Peier AM, Moqrich A, Hergarden AC, Reeve AJ, Andersson DA, Story GM, Earley TJ, Dragoni I, McIntyre P, Bevan S, Patapoutian A. TRP channel that senses cold stimuli and menthol. Cell 2002;108:705–15.
[62] Pertusa M, Madrid R, Morenilla-Palao C, Belmonte C, Viana F. N-glycosylation of TRPM8 ion channels modulates temperature sensitivity of cold thermoreceptor neurons. J Biol Chem 2012;287:18218–29.
[63] Quallo T, Vastani N, Horridge E, Gentry C, Parra A, Moss S, Viana F, Belmonte C, Andersson D, Bevan S. TRPM8 is a neuronal osmosensor that regulates eye blinking in mice. Nat Commun 2015;6:7150.
[64] Report of the international Dry Eye Workshop (DEWS). Ocul Surf 2007;5: 65–204.
[65] Rosenthal P, Borsook D. The corneal pain system. Part I: the missing piece of the dry eye puzzle. Ocul Surf 2012;10:2–14.
[66] Sittl R, Lampert A, Huth T, Schuy ET, Link AS, Fleckenstein J, Alzheimer C, Grafe P, Carr RW. Anticancer drug oxaliplatin induces acute cooling-aggravated neuropathy via sodium channel subtype Na(V)1.6-resurgent and persistent current. Proc Natl Acad Sci U S A 2012;109:6704–9.
[67] Stewart T, Beyak MJ, Vanner SJ. Ileitis modulates potassium and sodium currents in guinea pig dorsal root ganglia sensory neurons. J Physiol 2003;552:797–807.
[68] Tan JH, Ng EY, Acharya UR. Evaluation of tear evaporation from ocular surface by functional infrared thermography. Med Phys 2010;37:6022–34.
[69] Tan ZY, Donnelly DF, LaMotte RH. Effects of a chronic compression of the dorsal root ganglion on voltage-gated Na+ and K+ currents in cutaneous afferent neurons. J Neurophysiol 2006;95:1115–23.
[70] Thut PD, Wrigley D, Gold MS. Cold transduction in rat trigeminal ganglia neurons in vitro. Neuroscience 2003;119:1071–83.
[71] Tichy H. Humidity-dependent cold cells on the antenna of the stick insect. J Neurophysiol 2007;97:3851–8.
[72] Trost K, Skalicky M, Nell B. Schirmer tear test, phenol red thread tear test, eye blink frequency and corneal sensitivity in the guinea pig. Vet Ophthalmol 2007;10:143–6.
[73] Tsubota K, Monden Y, Yagi Y, Goto E, Shimmura S. New treatment of dry eye: the effect of calcium ointment through eyelid skin delivery. Br J Ophthalmol 1999;83:767–70.
[74] Veiga Moreira TH, Gover TD, Weinreich D. Electrophysiological properties and chemosensitivity of acutely dissociated trigeminal somata innervating the cornea. Neuroscience 2007;148:766–74.
[75] Viana F, de la Peña E, Belmonte C. Specificity of cold thermotransduction is determined by differential ionic channel expression. Nat Neurosci 2002; 5:254–60.
[76] Wasner G, Naleschinski D, Binder A, Schattschneider J, McLachlan EM, Baron R. The effect of menthol on cold allodynia in patients with neuropathic pain. Pain Med 2008;9:354–8.
[77] Xiao B, Dubin AE, Bursulaya B, Viswanath V, Jegla TJ, Patapoutian A. Identification of transmembrane domain 5 as a critical molecular determinant of menthol sensitivity in mammalian TRPA1 channels. J Neurosci 2008;28:9640–51.
[78] Xiao Y, Liang S. Inhibition of neuronal tetrodotoxin-sensitive Na+ channels by two spider toxins: hainantoxin-III and hainantoxin-IV. Eur J Pharmacol 2003;477:1–7.
[79] Yin K, Zimmermann K, Vetter I, Lewis RJ. Therapeutic opportunities for targeting cold pain pathways. Biochem Pharmacol 2015;93:125–40.
[80] Zhang X, Mak S, Li L, Parra A, Denlinger B, Belmonte C, McNaughton PA. Direct inhibition of the cold-activated TRPM8 ion channel by Gαq. Nat Cell Biol 2012;14:851–8.